AD-A069 112 VON KARMAN INST FOR FLUID DYNAMICS RHODE-SAINT-GENESE--ETC F/G 20/4
EFFECTS OF A TURBULENT FREE STREAM AND A WALL ROUGHNESS ON THE --ETC(U)
JUN 78 M MOELLER, D OLIVARI AFOSR-78-3584

UNCLASSIFIED VKI-1978-24 EOARD-TR-79-2 NL

| OF |
AD A069 112

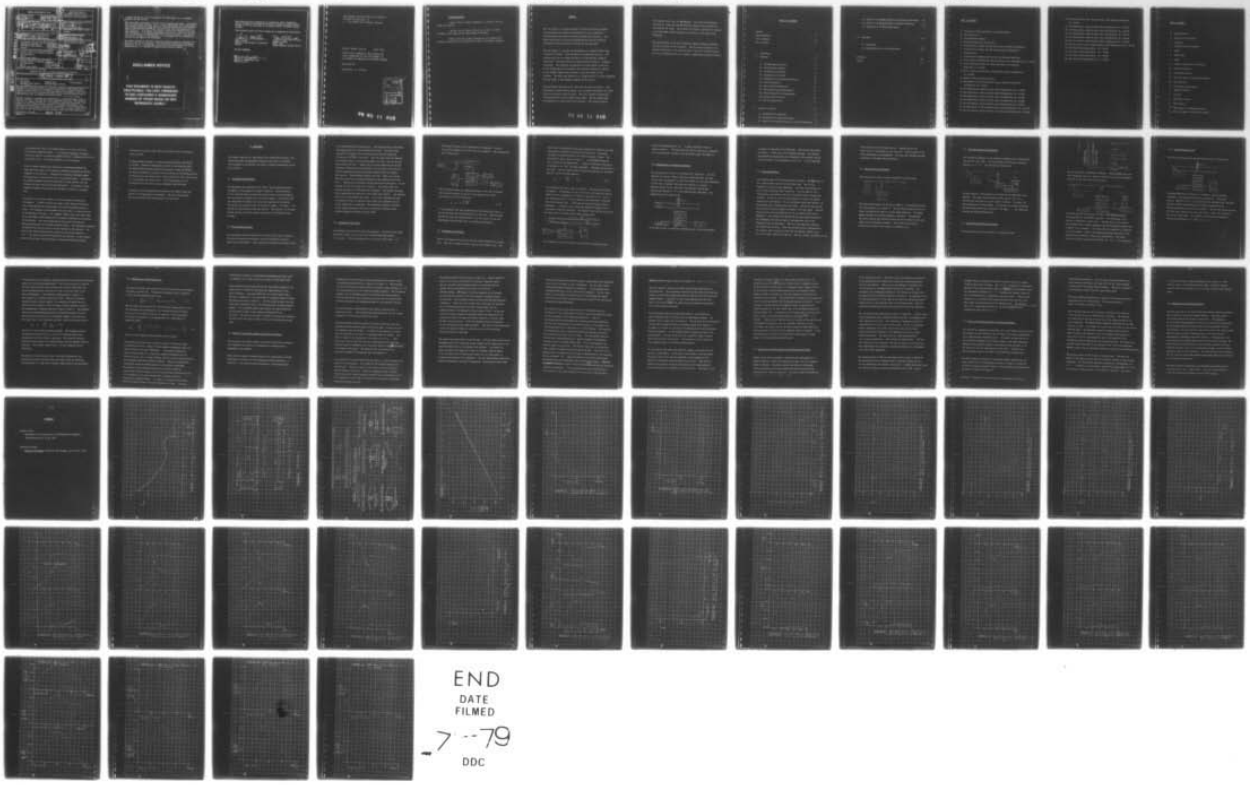

END
DATE FILMED
-7 -79
DDC

AD A069112

DDC FILE COPY

| REPORT DOCUMENTATION PAGE | READ INSTRUCTIONS BEFORE COMPLETING FORM |
|---|---|
| 1. Report Number: EOARD-TR-79-2 | 2. Govt Accession No.: TR-79-2 | 3. Recipient's Catalog Number |
| 4. Title (and Subtitle): EFFECTS OF A TURBULENT FREE STREAM AND A WALL ROUGHNESS ON THE FLOW NORMAL TO A CYLINDER AT SUBCRITICAL REYNOLD'S NUMBERS | 5. Type of Report & Period Covered: Final Report |
| | 6. Performing Org. Report Number: 1978-24 |
| 7. Author(s): Mark Moeller and D. Olivari | 8. Contract or Grant Number: AFOSR-78-3584 |
| 9. Performing Organization Name and Address: von Karman Institute for Fluid Dynamics, Chaussee de Waterloo, 72, 1640 Rhode Saint Genese, Belgium | 10. Program Element, Project, Task Area & Work Unit Numbers: 61102F, 2301-D1 |
| 11. Controlling Office Name and Address: European Office of Aerospace Research and Development, Box 14, FPO New York 09510 | 12. Report Date: June 1978 |
| | 13. Number of Pages: 71 |
| 14. Monitoring Agency Name and Address: European Office of Aerospace Research and Development, Box 14, FPO New York 09510 | 15. 68 p |

16. & 17. Distribution Statement

Approved for public release; distribution unlimited.

18. Supplementary Notes: VKI-1978-24

19. Key Words

Turbulence — Scaling Laws — Fluid Dynamics
Low Speed Wind Tunnels — Reynolds Number Effects

20. Abstract: The flow normal to a circular cylinder at subcritical Reynold's Numbers was investigated to determine the feasibility of using subcritical Reynold's Number model tests to determine supercritical behavior. This finds application in the area of predicting wind loads on structures with circular cross-sections such as chimneys and cooling towers. → next page

The flow normal to a cylinder was investigated in a Reynold's Number range of 90,000 to 170,000. Three different flow conditions were used. The reference case was of a smooth cylinder in a 0.5% turbulent intensity freestream. The second case was a smooth cylinder mounted in a turbulent freestream. The turbulence was generated by a grid placed in the flow. At the leading edge of the cylinder, the turbulent intensity was 12% and had an integral length scale the order of half the diameter of the cylinder. The third case tested was of

(Continued on reverse)

367 475

FORM 1473

LEVEL II
DDC
RECEIVED
MAY 30 1979
A

a rough cylinder in a quiet freestream. The mean height of the roughness elements was 250 microns.

The measurements were made in the VKI's L2A low speed wind tunnel. The measurements include static pressure, r.m.s. pressure fluctuation, wall shear stress, and velocity profiles at 90°. The r.m.s. pressure fluctuations were measured with a flush mounted Kulite probe. The wall shear stress was measured by a flush mounted hot film probe. The velocity profiles were measured with a hot wire anemometer. Also velocity measurements were made at 1/2mm, 1mm, and 2mm from the surface of the cylinder with flush mounted hot wires. The cylinder was rotated to generate the velocity at a fixed height from the cylinder as a function of the angle to the freestream.

The smooth cylinder in the quiet freestream exhibited behavior consistent with the data found in the literature. Both the smooth cylinder in the turbulent freestream and the rough cylinder in the quiet freestream showed some of the characteristics of a cylinder at supercritical Reynold's Numbers.


# DISCLAIMER NOTICE

THIS DOCUMENT IS BEST QUALITY PRACTICABLE. THE COPY FURNISHED TO DDC CONTAINED A SIGNIFICANT NUMBER OF PAGES WHICH DO NOT REPRODUCE LEGIBLY.

DDC FILE COPY

This report has been reviewed by the Information Office (EOARD/CMI) and is releasable to the National Technical Information Service (NTIS)/ At NTIS it will be releasable to the general public, including foreign nations.

This technical report has been reviewed and is approved for publication.

JOHN T. MILTON
Scientific and Technical Information Officer

ROBERT D. POWELL
Major, USAF
Flight Vehicles Liaison Officer

FOR THE COMMANDER

MICHAEL A. GREENFIELD, Ph.D.
Deputy Director

VON KARMAN INSTITUTE FOR FLUID DYNAMICS
CHAUSSEE DE WATERLOO, 72
B - 1640 RHODE SAINT GENESE, BELGIUM

PROJECT REPORT 1978-24 JUNE 1978

# *EFFECTS OF A TURBULENT FREE STREAM AND A WALL ROUGHNESS ON THE FLOW NORMAL TO A CYLINDER AT SUBCRITICAL REYNOLDS NUMBERS*

MARK MOELLER

SUPERVISOR : D. OLIVARI

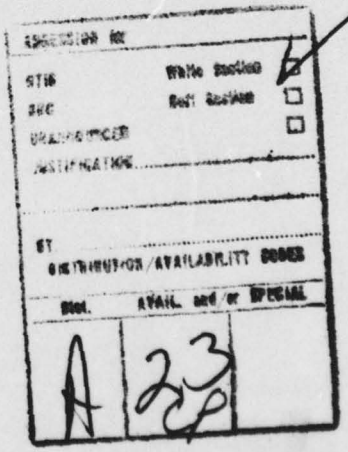


79 05 11 016

ACKNOWLEDGEMENT

I would like to thank Professor D. Olivari for his time and effort.

I would like to thank the US Air Force for their funding of my stay at the von Karman Institute.

Thanks also go to May Fitzpatrick for typing this project report and to my family for their continuous support.

## ABSTRACT

The flow normal to a circular cylinder at subcritical Reynold's Numbers was investigated to determine the feasibility of using subcritical Reynolds Number model tests to determine supercritical behavior. This finds applications in the area of predicting wind loads on structures with circular crossection such as chimneys and cooling towers.

The flow normal to a cylinder was investigated in a Reynolds Number range of 90,000 to 170,000. Three different flow conditions were used. The reference case was of a smooth cylinder in a 0.5% turbulent intensity freestream. The second case was a smooth cylinder mounted in a turbulent freestream. The turbulence was generated by a grid placed in the flow. At the leading edge of the cylinder, the turbulent intensity was 12% and had an integral length scale the order of half the diameter of the cylinder. The third case tested was of a rough cylinder in a quiet freestream. The mean height of the roughness elements was 250 microns.

The measurements were made in the VKI's L2A low speed wind tunnel. The measurements include static pressure, r.m.s. pressure fluctuation, wall shear stress, and velocity profiles at 90°. The r.m.s. pressure fluctuations were measured with a flush mounted Kulite probe. The wall shear stress was measured by a flush mounted hot film probe. The velocity profiles


79 05 11 016

were measured with a hot wire annemometer. Also velocity measurements were made at 1/2mm, 1mm, and 2mm from the surface of the cylinder with flush mounted hot wires. The cylinder was rotated to generate the velocity at a fixed height from the cylinder as a function of the angle to the freestream.

The smooth cylinder in the quiet freestream exhibited behavior consistant with the data found in the literature. Both the smooth cylinder in the turbulent freestream and the rough cylinder in the quiet freestream showed some of the characteristics of a cylinder at supercritical Reynold's Numbers.

# TABLE OF CONTENTS


| | |
|---|---|
| Abstract | i |
| Acknowledgements | iii |
| List of Figures | vi |
| List of Symbols | viii |
| 1. Introduction | 1 |
| 2. Experiment | 4 |
| 2.1 The Experimental Facility | 4 |
| 2.2 The Measurement Program | 4 |
| 2.3 Calibration of Hot Wires | 5 |
| 2.4. Calibration of Hot Films | 6 |
| 2.5 Determination of Freestream Conditions | 8 |
| 2.6 Flow Visualisation | 9 |
| 2.7 Static Pressure Measurements | 10 |
| 2.8 Fluctuating Pressure Measurements | 11 |
| 2.9 Flush Mounted Hot Wire Measurements | 11 |
| 2.10 Velocity Profiles at 90° | 13 |
| 2.11 Hot Film Measurements | 14 |
| 3. Analysis of Results | 15 |
| 3.1 Freestream Flow Conditions | 15 |
| 3.2 Determination of Drag Coefficients | 17 |
| 3.3 Results of the Smooth Cylinder in the Quiet Freestream | 18 |

3.4 Results of the Smooth Cylinder in the Turbulent Freestream 23

3.5 Results of the Rough Cylinder in the Quiet Freestream 25

3.6 Comparison of the Three Cases Tested 27

4. Conclusion 28

4.1 Conclusions 28

4.2 Recommendations for Future Experiments 28

References 30

Figures 31

LIST OF FIGURES


1. Variations of Drag Coefficient with Reynolds Number
2. Test Facilities
3. The Measurement Programs
4. Calibration Curve for the Hot Film
5. Velocity Profile Across the Test Section for the Quiet Configuration
6. Velocity Profile Across the Test Section behind the Turbulence Generating Grid
7. Nondimensional Frequency Spectrum for Grid Generated Turbulence
8. Static Pressure Distribution, Smooth Cylinder, Quiet Configuration, Re = 106,000
9. Static Pressure Distribution, Smooth Clylinder, Grid Generated Turbulence, Re = 104,000
10. Static Pressure Distributuion, Rough Cylinder, Quiet Configuration, Re = 106,000
11. Measured Values of Drag Coefficient
12. Measurements with Flush Mounted Hot Wires, Smooth Cylinder, Quiet Configuration, Re = 106,000
13. Flow Measurements, Smooth Cylinder, Quiet Configuration, Re = 93,000
14. Flow Measurements, Smooth Cylinder, Quiet Configuration, Re = 106,000
15. Flow Measurements, Smooth Cylinder, Quiet Configuration, Re = 117,000
16. Flow Measurements, Smooth Cylinder, Quiet Configuration, Re = 132,000
17. Flow Measurements, Smooth Cylinder, Quiet Configuration, Re = 167,000
18. Velocity Profile at 90°, Smooth Cylinder, Quiet Configuration, Re = 104,000
19. Flow Measurements, Smooth Cylinder, Grid Generated Turbulence, Re = 106,000

20. Velocity Profile at 90°, Smooth Cylinder, Grid Generated Turbulence, Re = 106,000

21. Flow Measurements, Rough Cylinder, Quiet Configuration, Re = 93,000

22. Flow Measurements, Rough Cylinder, Quiet Configuration, Re = 104,000

23. Flow Measurements, Rough Cylinder, Quiet Configuration, Re = 117,000

24. Flow Measurements, Rough Cylinder, Quiet Configuration, Re = 132,000

25. Flow Measurements, Rough Cylinder, Quiet Configuration, Re = 167,000

26. Velocity Profile at 90°, Rough Cylinder, Quiet Configuration, Re = 106,000

27. Wall Shear Stress Measurements. Re = 93,000

28. Wall Shear Stress Measurements. Re = 106,000

29. Wall Shear Stress Measurements. Re = 117,000

30. Wall Shear Stress Measurements. Re = 132,000

31. Wall Shear Stress Measurements Re = 167,000

## LIST OF SYMBOLS

| | |
|---|---|
| $C_d$ | Drag Coefficient |
| d | Diameter of the cylinder |
| f | Frequency |
| F | Measured Turbulence Spectrum |
| h | Height |
| H | Shape factor |
| L | Lenght |
| Lx | Integral length scale of Turbulence |
| $\Delta P$ | Pressure difference |
| $P_{atm}$ | Atmospheric pressure |
| $P_{r.m.s}$ | Root mean square of fluctuating pressure |
| Ps | Static pressure |
| $q_\infty$ | Freestream dynamic pressure |
| r | radius of cylinder |
| U | Velocity |
| U | Freestream velocity |
| U | Mean Velocity |
| $U^{\cdot 2}$ | Mean square of fluctuating velocity |
| $U_{r.m.s}$ | Root mean square of fluctuating velocity |

$\delta^*$ boundary layer displacement thickness

$\theta$ angle

$\Theta$ boundary layer momentum thickness

$\tau_w$ wall shear stress

$\nu$ dynamic viscosity

## 1. INTRODUCTION

The flow normal to a circular cylinder is frequently encounted in industrial fluid dynamics. One such case is wind loading on structures with circular crossections, such as chimneys and cooling towers. One tool used to gain more information about this type of flow is scale model tests in a wind tunnel. Because cooling towers and chimneys have large characteristic dimensions and the information on the wind loading is sought for high winds (40m/sec), the Reynold's Number, $\frac{U_\infty d}{\nu}$, of the full scale flow is very high. Unfortunately it is not possibe to do model tests at such high Reynold's Numbers. This paper is a preliminary investigation into model testing of chimneys and cooling towers at subcritical Reynold's Numbers.

In figure I the variations of drag coefficient with Reynold's Number is shown. One of the important features of this curve is the 'drag crisis' that occurs at a Reynolds Number of around $2 \times 10^5$. This drastic reduction in drag coefficient occurs because of a change in the boundary layer from laminar to turbulent. The turbulent boundary layer remains attached longer and so there is a better pressure recovery on the back face of the cylinder. Reynolds Numbers below the 'drag crisis' are said to be subcritical and Reynold's Numbers above the 'drag crisis' are said to be supercritical. The behavior of the flow in the two regions is considerably different. While wind loading on chimneys and cooling towers

are supercritical flows, it is often possible to do model tests only at subcritical Reynolds Numbers. It is therefore important to relate subcritical behavior to supercritical flow such that it behaves more like the supercritical flow. The second approach is used in practice.

There are several factors that influence at which Reynolds Number the drag crisis will occur, two of which are freestream turbulence and surface roughness of the cylinder. Increasing the freestream turbulence causes the drag crisis to occur earlier which is a desirable effect. Increasing the surface roughness causes the drag crisis to occur earlier, but also increases the base levels of the drag coefficient. In practice a surface roughness is applied to the model and the model is tested in a turbulent flow.

The effect of one surface roughness and one freestream turbulence was investigated. A smooth cylinder was tested in grid generated turbulence, and a rough cylinder was tested without the turbulence generating grid in place. For comparison the measurements were also made on a smooth cylinder in the abscence of the grid. The roughness elements used were sand, which had a mean height of 250 microns and were randomly distributed on the surface of the cylinder. This was accomplished by painting the cylinder and distributing the sand on the freshly painted surface. The freestream turbulence was generated by placing a grid in the flow upstream of the cylinder. The grid was 3mm thick aluminum and had a series of 4cm circular holes cut in it. The grid was placed 30cm upstream of the cylinder. At the leading edge of the cylinder, the grid produced a freestream turbulence of about

12% and had an integral length scale of the order of half the diameter of the cylinder.

The measurements were made in a range of Reynold's Numbers from 90,000 to 170,000. Because of the pressure loss due to the turbulence grid, the maximum Reynolds number tested with the grid in place was 106,000. The quantities measured include the static pressure and fluctuating pressure distributions, the wall shear stress, velocity profiles at 90°, and velocities at a fixed height from the cylinder. Two different types of flow visualisation were also used to gain information about the flow.

In chapter two the experiments are described and in chapter three the results of the experiments are discussed. The final section deals with the conclusions and recommendations for future work.

# 2. EXPERIMENT

This chapter begins with a description of the experimental facility, then briefly describes the experiments conducted, then goes on to describe the calibration of the sensors, and finally a detailed description of each test is given.

## 2.1 The Experimental Facility

The experiments were conducted in the VKI's L2A low speed wind tunnel. A schematic of this facility is shown in figure 2. The test section of the wind tunnel has a circular test section with a 0.3 meter diameter. The test section is divided into 3 one meter lengths. The cylinder used was 0.058 meters in diameter and was mounted spanning the wind tunnel. The cylinder was mounted so that it was free to rotate. In figure 3 the cylinder is shown mounted in the test section. The angle, $\theta$, is the angle between the axis of the test section and a point on the surface of the cylinder.

## 2.2 The Measurement Program

The measurements conducted broke down into three areas, shown in figure 3. The areas are pressure measurements, velocity measurements, and wall shear stress measurements. Static pressure measurements were made by means

of a flush mounted static pressure tap. Fluctuating pressure measurements were made by means of a flush mounted Kulite probe. The probes were rigidly mounted in the cylinder and by rotating the cylinder the variations of pressure with angle could be observed. Data were taken every five degrees. Two different types of velocity measurements were made. One set was with flush mounted hot wires. Special hot wires were constructed in the VKI Electronic Laboratory and flush mounted in the cylinder so that only the needles supporting the measuring filament remained above the surface, see figure 3. Three different heights were used, 1/2mm, 1mm, and 2mm. Both mean velocity and fluctuating velocities were measured as functions of $\theta$. Velocity and fluctuating velocity profiles were measured at $\theta = 90°$ by means of a hot wire mounted in a traverse. Wall shear stress was measured by means of a flush mount hot film probe. The cylinder was again rotated generating the variation of wall shear stress with $\theta$. Two different types of flow visualisation were used. An oil film technique was used to indicate the point of separation and a china clay technique was used to gain information on transition. The measurement program was designed to give enough information about the flow processes involved to make a detailed comparison between the three cases.

## 2.3 Calibration of Hot Wires

Two different sets of hot wire data were generated. One set was with flush mounted hot wires, the other was with a standard DISA probe mounted in a traverse. The same annemometer unit was used in both cases. In

both cases the output of the annemometer was linearised. The hot wires were calibrated in the VKI hot wire calibrator. The configuration used is shown below:

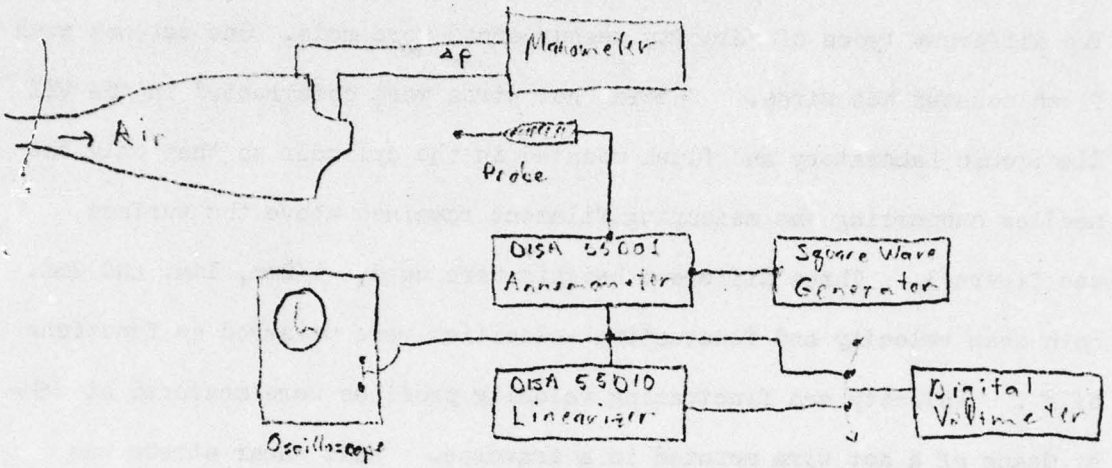


The difference between the stagnation pressure in the VKI calibrator and the static pressure at the exit were measured with a micro and related to the exit velocity by:

$$U \approx 4\sqrt{\Delta p} \qquad 2.1$$

It was determined that when calibrating the flush mounted hot wires, it was best to mount the wires perpendicular to the flow. When the flush mounted hot wires were mounted normal to the flow, there was too much interference from the probe mount to calibrate them properly.

## 2.4 Calibration of Hot Films

The hot film sensor used was a thin film of platinum deposited on a glass base. The film was three milimeters long and one milemeter wide. The

glass rod it was deposited on was three milemeters in diameter, the leads were painted in grooves on the side of the glass rod. For proper insulation, the glass rod had to be fixed in a ceramic sleeve. The configuration used is shown in figure 3. A DISA 55D01 annemometer unit was used for the measurements. A special calibration setup had to be arranged in the VKI low speed laboratory. The probe was mounted in a long pipe. The wall shear stress was calculated assuming well developed pipe flow by the following equation:

$$\tau_w = \left(\frac{\Delta p}{L}\right)\left(\frac{r}{2}\right) \qquad 2.2$$

The calibration facility is shown in figure 2. The pipe is 0.06 meter in diameter. To eliminate any swirl in the flow, the pipe had a setting chamber with flow straighteners mounted on the front of it. It was then determined that 80 - 100 pipe diameters were necessary to establish fully developed pipe flow. The probe was mounted 100 pipe diameters downstream. In order to get a accurately measurable pressure loss, a long length of pipe was necessary. The length of pipe used was six meters. The setup used to calibrate the hot film is shown below:

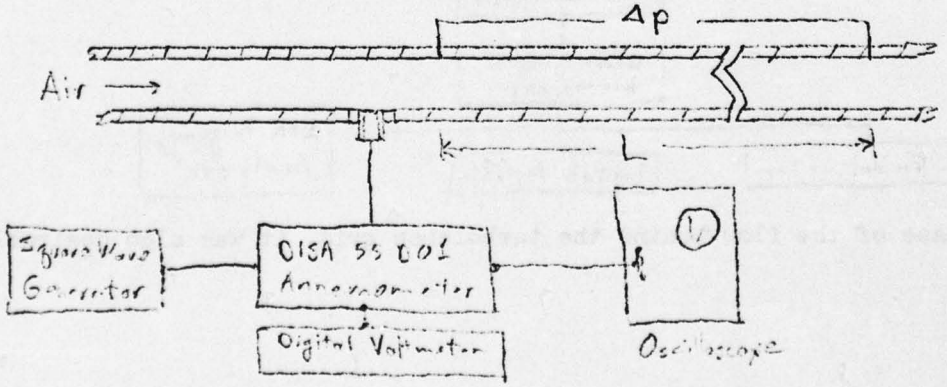


The resistance of the hot film probe was 15 Ω and the overheating ratio

used in the annemometer was 1.5. A sample calibration curve is shown in figure 4. The data taken with the hot film was not linearised so it was necessary to reduce it by hand using a graph like figure 4.

## 2.5 Determination of Freestream Conditions

The cylinders were tested in two different flow conditions. One flow condition was the flow behind a turbulence generating grid, the other was the quiet configuration in which the original flow was left undisturbed. In both cases a standard DISA probe was mounted in a traverse. A traverse was made of the wind tunnel test sections, and the mean velocity and turbulent intensity were measured every centimeter. The configuration used is shown below:

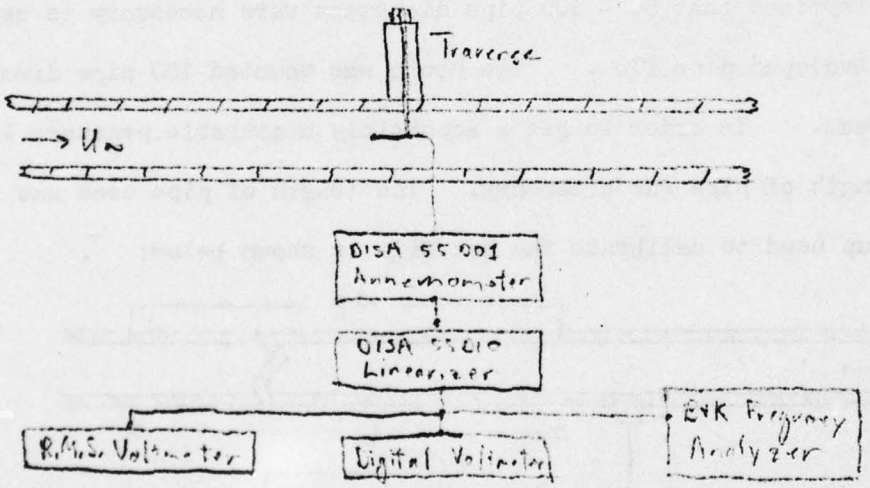


In the case of the flow behind the turbulence grid, it was also desirable

to measure the spectrum of the turbulence. This was done by putting the linear[illegible] output into a B+K frequency analyzer. The spectrum was generated by varying the center frequency of the analyzer, and the analyzer bandwith, and measuring the r.m.s. power in that bandwidth.

## 2.6 Flow Visualisations

Two different types of flow visualisations were made. The ~~type~~ two types of flow visualisations were oil film and china clay. The oil film technique was used to locate separation. The china clay technique was used to gain information about transition. For both types of flow visualisation, the cylinder used had to be painted black to obtain good contrast. For the oil film flow visualisation, a special oil pigment mixture had to be prepared. The oil and pigment were mixed together and then thinned until a usable mixture was found. The oil was then painted on the cylinder and the cylinder was placed in the wind tunnel. The wind tunnel was then run long enough for the oil to collect at the line of separation. The cylinder was removed from the wind tunnel; the pattern was photographed and then the angle of the separation line to the stagnation point was determined. The use of the china clay technique was slightly more involved. First the cylinder had to be painted black for contrast, then a coating of china clay was applied, finally a very even coat of Ethyl Benzoate was applied. Then the cylinder was mounted in the

wind tunnel and the wind tunnel was run. Running time for the tunnel had to be determined by trial and error. The end result of the flow visualisation was photographed. The china clay technique provides information on boundary layer transitions.

## 2.7 Static Pressure Measurements

The set up for the static pressure measurements is shown below:

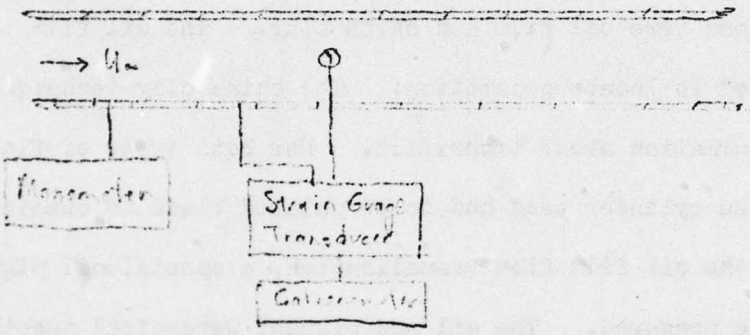


The flush mounted static tap was 1mm in diameter. The difference between the static pressure at an angle $\theta$ and the static pressure in the wind tunnel was measured by means of a strain gauge transducer. The strain guage transducer was calibrated against a monometer. The monometer was used to measure the difference btween the static pressure in the wind tunnel and the atmospheric pressure. This value was monitored to maintain the velocity in the tunnel at a constant level.

## 2.8 Fluctuating Pressure Measurements

The fluctuating component of the pressure was measure with a flush mounted Kulite probe ( CQ - 080). The Kulite probe was statically calibrated against a manometer . The test setup is shown below:

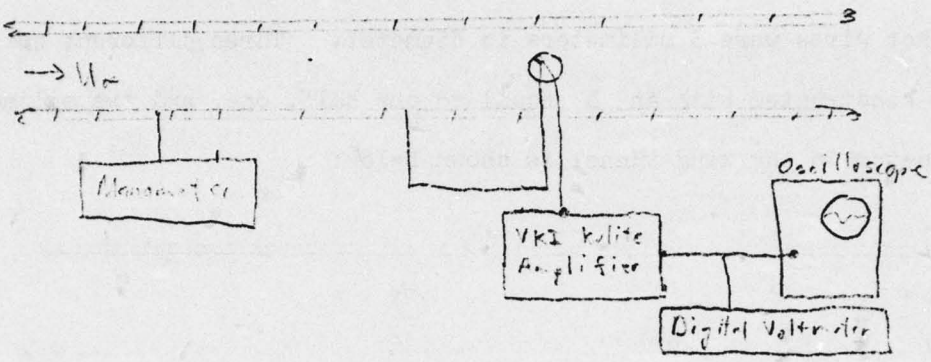


The back pressure on the diaphram of the probe was the freestream static pressure. The signal form the probe was fed into the VKI Kulite Amplifier and then read on a r.m.s. digital voltmeter. The signal was also displayed on the oscilloscope. The cylinder was rotated to generate the fluctuating pressure as a function of the angle, . The freestream velocity was maintained constant by

## 2.9 Flush Mounted Hot Wire Measurements

The flush mounted hot wires are shown in a schematic below:

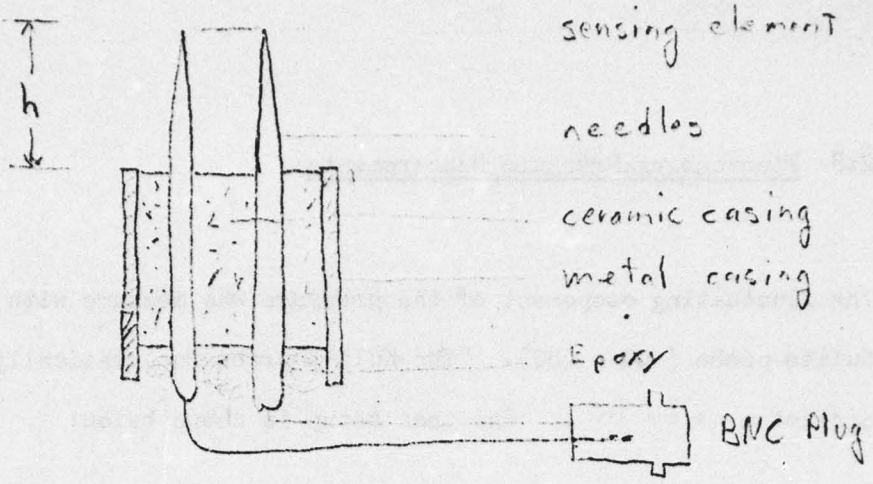


The hot wires were 3 milimeters in diameter. Three different hot wires were constructed with an h equal to one half, one, and two milimeters. The setup in the wind tunnel is shown below:

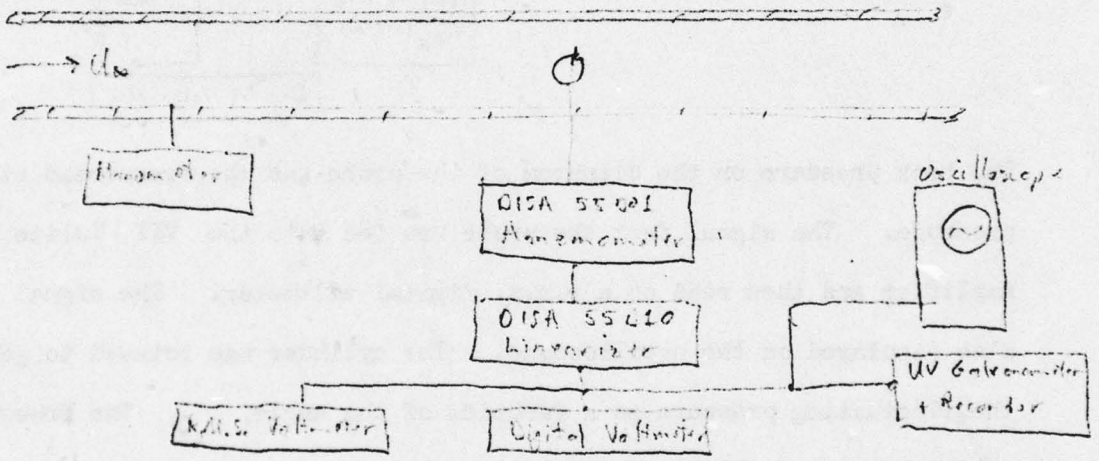


the output form the hot wire was fed into a DISA 55D01 annemometer and linearised by a DISA 55010 linearizer. The calibration of the hot wire is discussed in section 2.3. The mean value of the velocity was determined from a digital voltmeter, and the fluctuating component from a digital r.m.s. voltmeter. The output from the linearizer was displayed on an oscilloscope. When it was considered desirable the output of the linearizer was recorded by a Ultraviolet galvanometer. The tunnel speed was maintained constant by monitoring $P_{atm} - P_{static}$ with a manometer.

## 2.10 Velocity Profiles at 90°

The setup for measuring the velocity profiles at 90° is shown below:

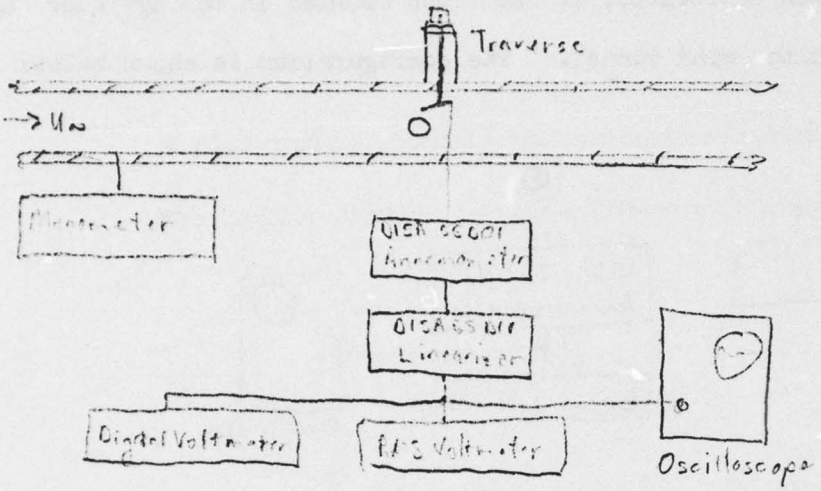


A standard DISA probe was mounted in a traverse. The hot wire was calibrated by the procedure described in section 2.3. The output from the DISA 55 D01 Anemometer unit was fed into the DISA 55 D10 linearizer. The mean velocity was determined from a digital voltmeter and the fluctuating componet form an r.m.s. voltmeter. The hot wires were positioned at 90° and then traversed until the wire burned. After the wire burned the zero was established. The velocity in the tunnel was maintained constant by monitoring Pitot head with a manometer.

## 2.11 Hot Film Measurements

The hot film and its calibration are described in section 2.4. After the hot film was calibrated, it was flush mounted in the cylinder and then mounted in the wind tunnel. The configuration is shown below:

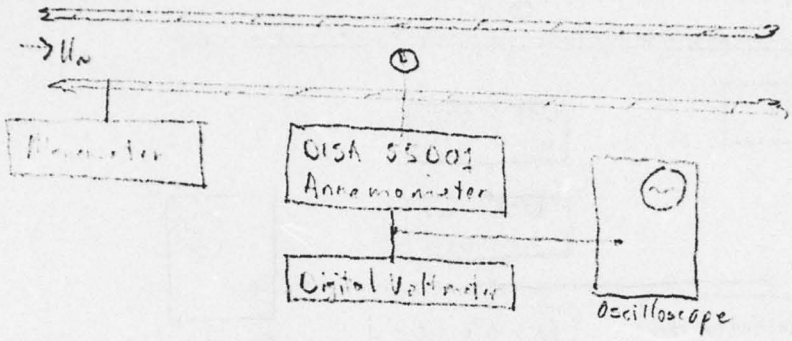


The output of the annemometer until was read on a digital voltmeter, and also displayed on a storage scope. When it was desired the image on the screen could be photographed with a scope camera. The data was reduced by hand using the calibration curve generated in section 4. $P_{atm} - P_{test}$ was monitored to maintain the wind tunnel at a constant speed.

# 3. ANALYSIS OF RESULTS

In this chapter the results of the experiments described in Chapter Two are discussed. In section 3.1, the determination of the freestream conditions are discussed. In section 3.2, the results of the static pressure measurements are discussed. Then in sections 3.3 to 3.5 the results of the measurements on the smooth cylinder in the quiet freestream, the smooth cylinder in the grid generated turbulence, and the rough cylinder in the quiet freestream are discussed. In section 3.6, the results of the three cylinders are compared.

## 3.1 Freestream Flow Conditions

The measurements of the freestream conditions in the wind tunnel was discussed in section 2.5. The freestream conditions for the wind tunnel in the quiet configurations are shown in figure 5. The core of the wind tunnel shows very nearly a straight line, the turbulent intensity varies across the width of the wind tunnel. The turbulent intensity varies from 0.5 % to 1.8%, these values are reasonable for the configuration of the wind tunnel used. Near the walls of the wind tunnel the mean velocity decreased and the turbulent intensity increased as the probe moved closer to the wall.

The mean velocity and turbulence intensity profiles were measured 30centimeters behind the turbulence generating grid. The results are shown in figure 6. The mean velocity profile shows somewhat more variation then before and starts decreasing farther from the wall than in the wind tunnel in the quiet configuration. The turbulent intensity profile, however, is quite regular at a turbulent intensity of 12%. Because the turbulent intensity profile is quite regular it is reasonable to assume that the spectrum of the turbulence does not change too much from point to point. The nondimensional frequency spectrum is shown in figure 7. The frequency spectrum was nondimensionalised using the freestream velocity, the mean square velocity fluctuation, and the integral length of the turbulence. The lenght scale of the turbulence was found from the following relation:

$$L_x = \frac{\bar{u}}{4\,\bar{u}^2} \lim_{n \to 0} F(n)$$

where F(n) is the measured frequency specturm. The frequency spectrum was checked by fitting lines to a plot of the frequency spectrum and integrating to find the turbulent intensity. The turbulent intensity calculated by this method was in good agreement with the measured turbulent intensity. The integral length scale, L of the turbulence was 2.5 centimeters.

The results of this section are that in the quiet configuration the freestream turbulent intensity varies from 0.5 to 1.8%, and behind the turbulence grid it is 12% with an integral length scale of 2.5 centimeters.

## 3.2 Determination of Drag Coefficients

The drag coefficients were calculated from the static pressure measurements described in section 2.7. The pressure distribution can be integrated to find the drag coefficient as follows:

$$C_D = \left(\frac{2}{q_\infty d}\right) \int_0^\pi P(\theta) \cos\theta \, d\theta \qquad 3.1$$

The data that were taken were (Po - Ps) for every 5 degress from 0 to 180. The freestream static pressure, Ps, is a constant and does not change the value of the integral in Eq 3.1 so using (Po - Ps) is acceptable. The integral in Equation 3.1 was approximated by a trapezoidal rule quadrature scheme:

$$C_D = \frac{\Delta\theta}{q_\infty} \left[ \frac{P(0) - P(\pi)}{2} + \sum_{n=1}^{35} P(\theta_n) \cos\theta_n \right] \qquad 3.2$$

The use of this quadrature scheme yielded reliable results.

The pressure distributions for a Reynold's Number of 106,000 are shown in figures 8,9, and 10. Figure 8 is the pressure distribution around the smooth cylinder in the quiet freestream. The pressure distribution shown is fairly typical of a subcritical pressure distribution and the calculated $C_D$ of 1.38 is in good agreement with the values of drag coefficient for cylinders at subcritical Reynold's Numbers. Figure 9 is the pressure distribution around the smooth cylinder in the turbulent freestream. The behavior of the pressure distribution is similar to those of supercritical Reynold's Numbers and the calculated drag coefficient of 0.38 is in agreement with the drag coefficients of smooth cylinder at supercritical Reynolds Numbers. In figure 10 the pressure distribution around the rough cylinder in the quiet freestream is shown. The drag

coefficient calculated for this pressure distribution was 0.99, which is reasonable for a rough cylinder at a Reynold's Number of 106,000.

Drag coefficients were calculated for four more Reynolds Numbers in the range 90,000 to 170,000 for the smooth and rough cylinders in the quiet freestream. The drag coefficient for a smooth cylinder in a turbulent freestream was also calculated at a Reynolds Number of 93,000. The results are shown in figure 11. For the smooth cylinder, the drag coefficient ranged from 1.39 to 1.26 decreasing with increasing Reynolds Numbers. In the Reynolds Number range tested, the drag coefficients for the smooth cylinder in the turbulent freestream did not vary much. The value for the smooth cylinder in the turbulent freestream was 0.38 and for the rough cylinder in the quiet freestream $C_d$ was equal to 1.0.

### 3.3 Results of the Smooth Cylinder in the Quiet Freestream

The flow around the smooth cylinder in the quiet freestream was measured as a reference case and then two parameters were changed and the measurements were repeated.

There were five Reynold's Numbers tested in the range 90,000 to 170,000. The results of the oil film flow visualisation showed separation at around 72°. The static pressure distribution, fluctuating pressure

distribution, and body centered velocity measurements are shown in order of increasing Reynolds Nulber in figure 13 to figure 17. The difference between the local static pressure and the freestream static pressure, $P_\theta - P_s$ are nondimensionalised on the freestream dynamic pressure. The fluctuating pressure is also nondimensionalised on the freestream dynamic pressure. Both the mean velocity and fluctuating velocities from the body centered velocity measurements are nondimensionalised on the freestream velocity.

The static pressure distributions all show behavior characteristic of subcritical flows. The corresponding drag coefficients are also in good agreement with other data on subcritical flows.

The body centered velocities measured with flush mounted hot wires were measured at three different heights from the cylinder: one half, one, and two millimeters from the surface. In figure 12 the results of all three hot wire measurements are shown for a Reynolds Number of 106,000. Also shown is figure 12 in the potential flow solution of $2 \sin\theta$ . From figure 12, it can be seen that the use of three different hot wires did not yeild much new information and so only the results of the 1mm measurements are presented in the body of the report. The deviation from the potential flow solution is because of the boundary layer and separation .

The variation of the mean velocity with the angle, $\theta$ , shown in figure 13 to figure 17 is very regular. Up to about 60° the velocity increased with increasing $\theta$. Looking at figure 14, the velocity levels off when the pressure gradient levels off. Behind the separation point, the mean velocity has little meaning because no direction can be associated with it. It is interesting to note that the magnitude of the mean and fluctuating velocities are about the same.

The velocity profile at 90° is shown in figure 18. Because separation occurs at 72°, the velocity profile is through a separated region. The mean velocity starts decreasing about 2.3 milimeters from the surface and the zero crossing is at about 1.2 milimeters from the surface. In figure 18 only the magnitude of the velocity is shown and the direction of the flow inside the separated region is not known. The fluctuating velocity profile provides some additional information. Before the mean velocity starts decreasing the magnitude of the fluctuating velocity is 7% which is much higher than the freestream value in the abscence of the cylinder of 0.4%. As the mean velocity decreases throught the separated regions the magnitude of the fluctuating velocity increases and reaches a maximum at the point where the mean velocity is zero. Inside the separated region the magnitude of the fluctuating velocity again decreases. The result of this measurement is that the separated region is very small and that the fluctuating velocity intensity is very high.

Wall shear stress measurements were also made. The wall shear stress was non-dimensionalised by the freestream dynamic pressure and the square root of the Reynold's Number based on the radius of the cylinder. The results are shown in figure 27 to figure 31 in order of increasing Reynolds Number. In all the cases the wall shear stress starts at a low value, grows to a maximum and decreases until separation. The wall shear stress measurements provide information on the point of separation. Using the wall shear stress

data for this purpose only yeilds a range of angles because the annemometer output did not decrease to zero at separation. The wall shear stress also provides some information on transition. If the boundary layer undergoes transition, the wall shear stress increases. The wall shear stress is very regular, the china clay flow visualisation alos showed very little and so there is laminar separation around 75° for the cylinder at subcritical Reynolds Numbers.

The quantities that provide additional useful information about the characture of flow around smooth cylinder at subcritical Reynold's Numbers are the measurement of the fluctuating quantities. Both the fluctuating pressure measurements and fluctuating velocity measurements made with the flush mounted hot wire show that most of the energy in the fluctuating quantities is contained in a single frequency. The frequency was determined by using a storage oscillscope and counting the periods and determining the total time of a trace. The frequencies determined this way were nondimensionalized on cylinder diameter and freestream velocity, which is a Strouhal Number, $\frac{fd}{U}$. In all cases measured the Strouhal Number was near 0.23. The Strouhal Number for vortex shedding from a cylinder is reported in the literature as 0.21. The error in the measured value is probably due to an error in determination of the frequency. The nearly perfect sine waves also showed up in the wall shear stress measurements and were photographed with an oscilloscope camera. ~~Figure 32 and Figure 33 are~~ were Sample traces of hot wire output obtained with an ultraviolet lightspot galvanometer. At the leading edge of the cylinder there is interference from the vortex shedding on the two faces of the cylinder.

~~Figure 34 are~~ Some sample traces in the region were obtained in this region.

The other important thing to note about the fluctuating quantities are their magnitude. The fluctuating velocities are about 5% of the freestream velocity and the fluctuating pressure goes as high as 50% of the freestream dynamic pressure. The result is that vortex sheeding from the front face of the cylinder ~~cases~~ causes very large velocity and pressure fluctuations at the vortex sheeding frequency.

The fluctuating pressure and fluctuating velocity also showed some unusual behaviour that is believed to be an experimental anomaly. The behaviour can be clearly seen in figure 12. The intensity of the fluctuating velocity shows a sudden dip before increasing rapidly after separation. In figure 14 to figure 17, the dips in fluctuating pressure and fluctuating velocity correspond. As the Reynolds Number increases the width of the dip increases. The dip did not occur for a Reynold's Number of 93,000 and so some critical value exists. At the point of the dip, there are also irregular steps in the static pressure profile.

It is my opinion that these dips represent a change in the mean flow and are not a local effect. On the face of the cylinder a line was etched that could just be felt with the fingertips so the roughness on the cylinder is very small, much less than 0.1 milimeters. This line was etched on the cylinder for mounting the probes in the proper position and for positioning the cylinder in the test section. The line is a two

dimensional roughness element on a very smooth cylinder and two - d roughness is generally worse than an isolated three - d roughness element. As the cylinder is rotated the two- d roughness element changes position. At some critical Reynolds Number and position, the roughness element causes a change in the mean flow such that separation is moved to the back face of the cylinder. This would cause a reduction in the intensities of the fluctuating pressure and fluctuating velocity as observed. As the cylinder is rotated further the roughness element is moved into the separated region and the flow relaxes back to an undisturbed subcritical Reynolds Number flow. The position of the leading edge of the dip can be seen to occur at a Reynolds Number based on arc length, $\frac{(r\theta)U_\infty}{\nu}$, of 135,000. Whether or not this dip is due to a change in the mean flow can be determined by etching a line on a cylinder, mounting it in the wind tunnel, and using a rake in the wake, compute the drag coefficient of the cylinder as the angle of the roughness element is changed. If the separation point does move to the back face of the cylinder, a large change in the drag coefficient should occur.

## 3.4 Results of the Smooth Cylinder in the Turbulent Freestream

Because of the speed limitations a complete set of measurements of a smooth cylinder in a turbulent freestream was made only for a Reynolds Number of 106,000. The static pressure distribution, fluctuating pressure distribution and one milimeter high flush mounted hot wire measurements are shown in figure 19. The static pressure distribution is very similar to a distribution

for a supercritical flow. The mean velocity also behaves very regularly. On the upstream face the fluctuating velocity and fluctuating pressure are also very regular. There was not one frequency to associate with the fluctuation so a Strouhal Number could not be determined. The magnitude of the fluctuating component of the velocity in the same order of magnitude as the freestream velocity fluctuation. The magnitude of the fluctuating pressure is of the order of one fourth the freestream dynamic pressure which is less than half that of the reference case. Both the fluctuating pressure and velocity increased near the point of separation.

The wall shear stress measurements are shown in figure 28. The wall shear stress measurements show a separation bubble near 95°, a reattachment and a final separation near 125°. This conclusion is supported by both flow visualisations, the oil film and the china clay. The oil film technique showed a separation line at 92°, which is too early for the static pressure distribution measured, but in agreement with the wall shear stress measurements. The china clay flow visualisation showed a line of black surrounded by white regions of attached flow. The back face behind the final separation line was also black, so the china clay flow visualisation also indicates a separation followed by a reattachment at 95° and a final separation.

The velocity profile at 90° was also measured and is shown in figure 20. The velocity profile is a boundary layer in this case because the flow is still attached to the cylinder at this point. Outside the boundary layer the turbulent intensity is near the freestream value of 12%. As the

boundary layer is traversed the turbulent intensity rises to a maximum of 20% and then falls off again. The momentum thickness $\theta$, displacement thickness $\delta^*$, and shape factor H, $H = \frac{\delta^*}{\theta}$ were ~~completed~~ computed for the boundary layer. The displacement thickness and momentum thickness are integral quantities and were approximated by a trapizoidal quadrature scheme. There are some errors due to the difficulties in positioning the probe, and due to the small number of points measured in the boundary layer. The computed result was a displacement thickness of .29 milimeters and momentum thickness of .14mm which have a corresponding shape factor of H = 2.1.

## 3.5 Results of the Rough Cylinder in the Quiet Freestream

The cylinder was roughened by using sand with a mean dimension of 250 microns. The cylinder was then mounted in the wind tunnel in the quiet configuration with a .5% freestream turbulence level. The rough cylinder was run at the same Reynolds Numbers as the smooth cylinder in the quiet freestream. Because of the roughness elements on the surface of the cylinder, it was not possible to do flow visualisation in this case. Otherwise the same measurements made on the other two cylinders were repeated again.

The static pressure distribution, fluctuating pressure distribution, and flush mounted hot wire measurements are shown in figure 21 to figure 25 in order of increasing Reynolds Number. The wall shear stress measurements are shown in figure 27 to figure 31.

The point of separation occurs around 100° as determined from the wall

shear stress measurements. The wall shear stress measurements also show transition occuring in the range of 30° to 45°, with transition occuring earlier for higher Reynolds Numbers. The way it is detected is the change in slope of the wall shear stress curve.

The static pressure distribution is reasonable for the separtion point predicted by the wall shear stress. The drag coefficient of around 1.0 is also a reasonable value.

The fluctuating pressure and fluctuating velocities on the front face of the cylinder also have a characteristic frequency. The frequency was determined the same way as in the case of the smooth cylinder in the quiet freestream. The Stouhal Number associated calculated for the rough cylinder was 0.25. The collapse of the data was not as good as that for the reference case. The difference between the smooth cylinder and the rough cylinder, 0.25 compared to 0.23, is considered large enough to be real and not just due to experimental error. The magnitude of the fluctuating quantities is smaller than the previous case. The fluctuating pressure on the front face of the cylinder is only 10% of the freestream dynamic pressure and the fluctuating velocity is only 1% of the freestream veloci

The velocity profile at 90° is again a boundary layer. The data were handled in the same way on the data for the smooth cylinder in the turbulent freestream. The displacement thickness calculated is .61 milimeters, the momentum thickness is .25 milimeters, therefore the shape factor is H = 2.4. The turbulent intensity profile is also shown in figure 26. The value

of turbulent intensity outside the boundary layer is only 1 to 1.5% which is close to the freestream value of .5%. Inside the boundary layer the turbulent intensity rises to a maximum of 9% and then decreases again.

### 3.6 Comparison of the Three Cases Tested

The smooth cylinder in the quiet freestream exhibited behaviour consistent for a cylinder at subcritical Reynolds Numbers. Separation occured on the front face of the cylinder at around 75°. The roughening of the surface caused separation to move to the back face of the cylinder. The fluctuating pressure and fluctuating velocities measured with the flush mounted hot wires were much lower for the case of the rough cylinder. Both the smooth cylinder and rough cylinder in the quiet flow had characteristic frequencies associated with them. The frequency of the rough cylinder was slightly higher than that of the smooth cylinder. The Smooth cylinder in the turbulent flow did not have an easily identified frequency associated with it, by taking spectra perhaps a peak will occur associated with the vortex shedding. The smooth cylinder in the turbulent flow had levels of fluctuating pressure and velocity that can be attributed to the freestream turbulence.

The static pressure distributions and associated drag coefficients are reasonable for all the cases studied. Also the velocity profiles at 90° are qualitatively reasonable for the flows measured.

# 4. CONCLUSIONS

## 4.1 Conclusions

1. The addition of surface roughness on the cylinder caused the separation point to move from the front face of the cylinder to the back face and the drag coefficient changed from 1.38 to 1.0.

2. Placing the smooth cylinder in a turbulent freestream caused the separation point to move from the front face of the cylinder to the back face and the drag coefficient changed from 1.38 to 0.38.

3. The static pressure distribution and associated drag cofficient for the smooth cylinder in the turbulent freestream is similar to that of a smooth cylinder at a supercritical Reynolds Number.

## 4.2 Recommendations for Future Experiments

1. It would be useful for comparison purposes to run the entire set of measurements on a smooth cylinder at a supercritical Reynolds Number.

2. It would be useful to combine the effects of surface roughness and freestream turbulence to be closer to actual conditions used in modeling.

3. It would be useful to run tests in different freestream turbulences and with different surface roughness.

4. In the case of the smooth cylinder in the turbulent freestream, spectra could be measured to see if there is a frequency associated with vortex sheeding.

5. The hypothesis presented in section 3.3 could be tested. A smooth cylinder with a very fine two - d roughness element could be tested to see if there is a significant effect due to the roughness element.

## REFERENCES

Geremia, John O.

"Experiments on the Calibration of Flush Mounted Film Sensors", DISA Information No. 13, May 1972.

Schlichting, Herman

Boundary Layer Theory, McGrow-Hill Book Company, Inc, New York, 1960.

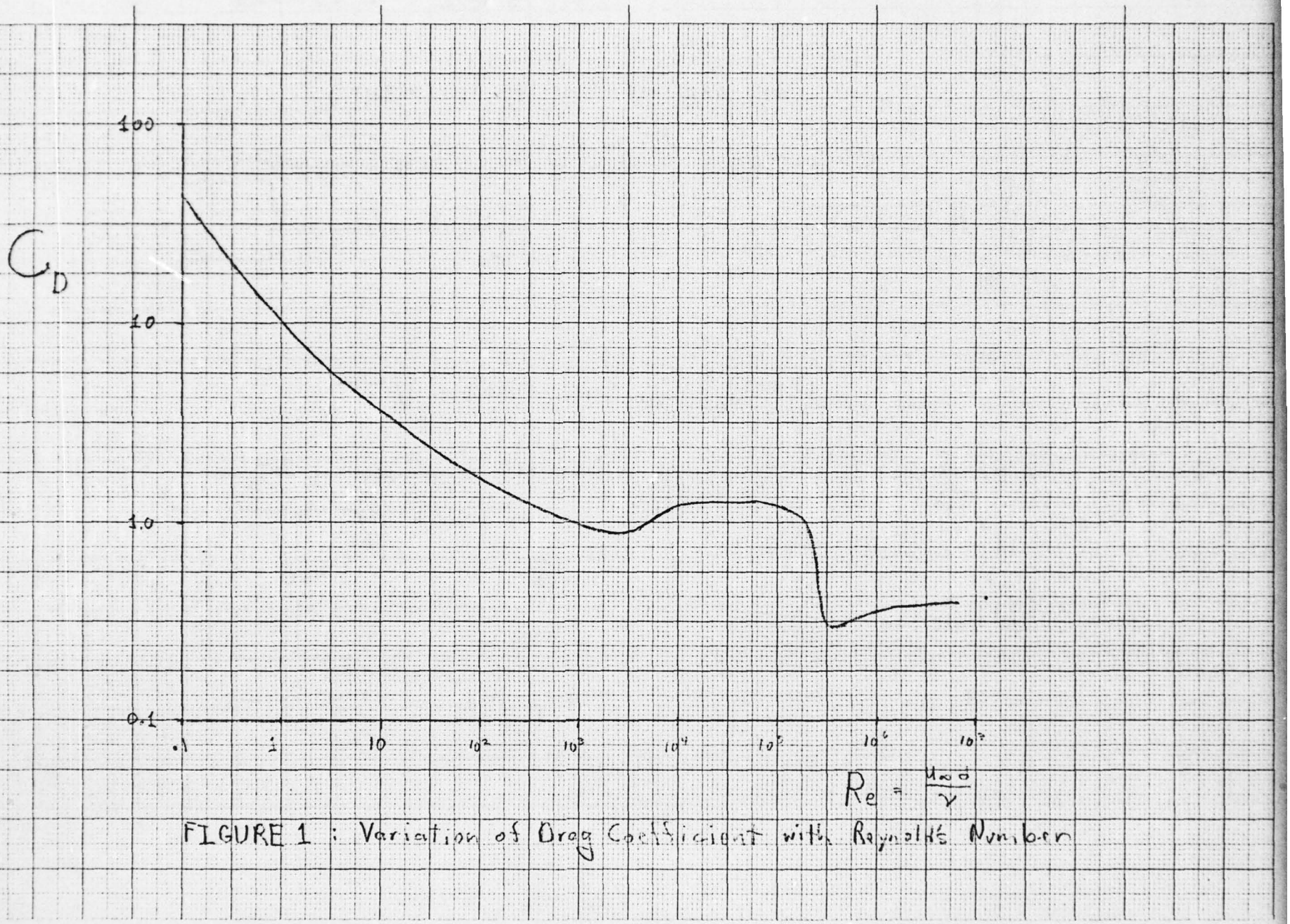


FIGURE 1 : Variation of Drag Coefficient with Reynolds Number

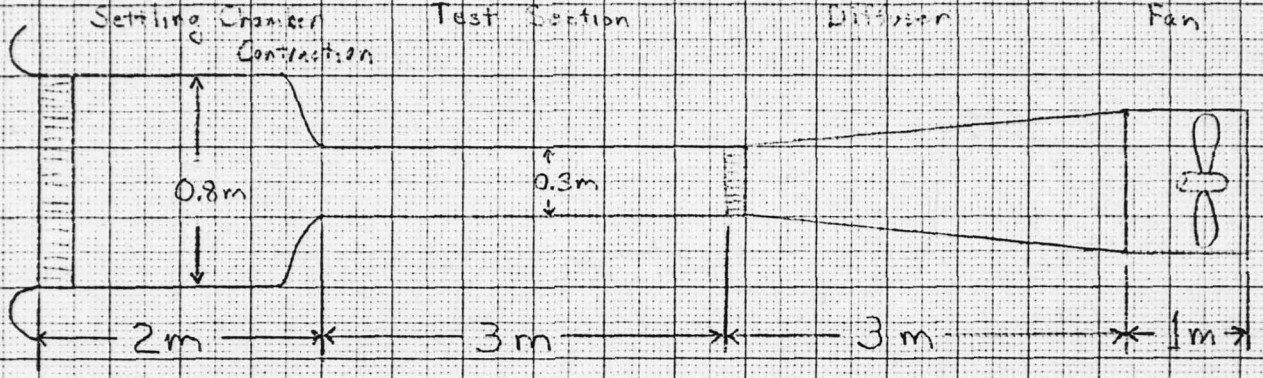


L2A Low Speed Wind Tunnel

Calibration facility for Hot Film

FIGURE 2 : Test Facilities

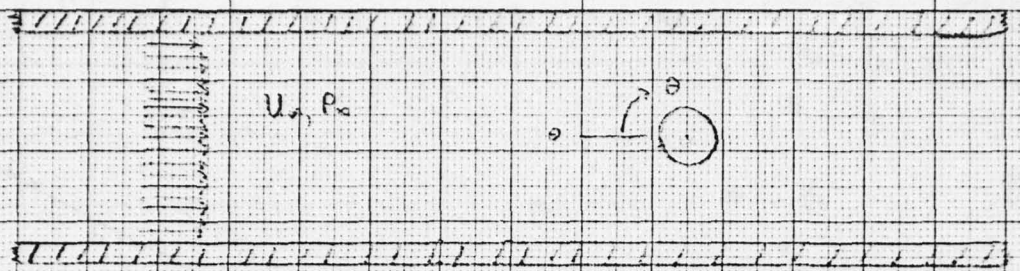


Cylinder Mounted in the Wind Tunnel

# FIGURE 3: MEASUREMENT PROGRAM

## PRESSURE MEASUREMENTS

### I. STATIC PRESSURE:

FLUSH MOUNTED STATIC PRESSURE TAP

### II. FLUCTUATING PRESSURE:

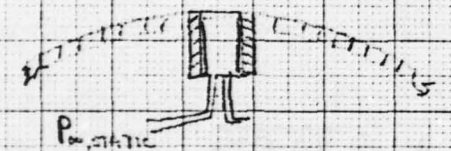


FLUSH MOUNTED KULITE PROBE

## VELOCITY MEASUREMENTS

### I. BODY CENTERED VELOCITIES:

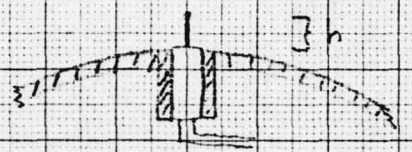


FLUSH MOUNTED HOT WIRE
h = ½ mm, 1 mm, 2 mm

### II. VELOCITY PROFILES:

HOT WIRE MOUNTED IN A TRAVERSE

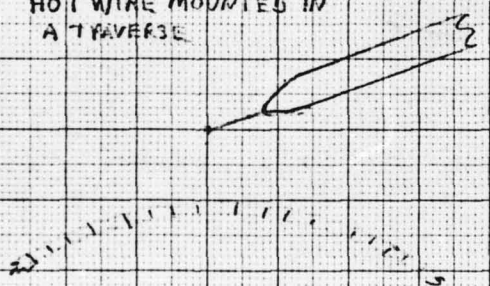

## WALL SHEAR STRESS MEASUREMENTS

### I. WALL SHEAR STRESS:

FLUSH MOUNTED HOT FILM PROBE

### II. FLOW VISUALIZATIONS

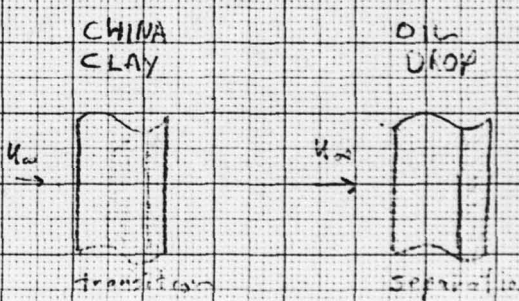

FIGURE 4 : Calibration Curve for the Helium

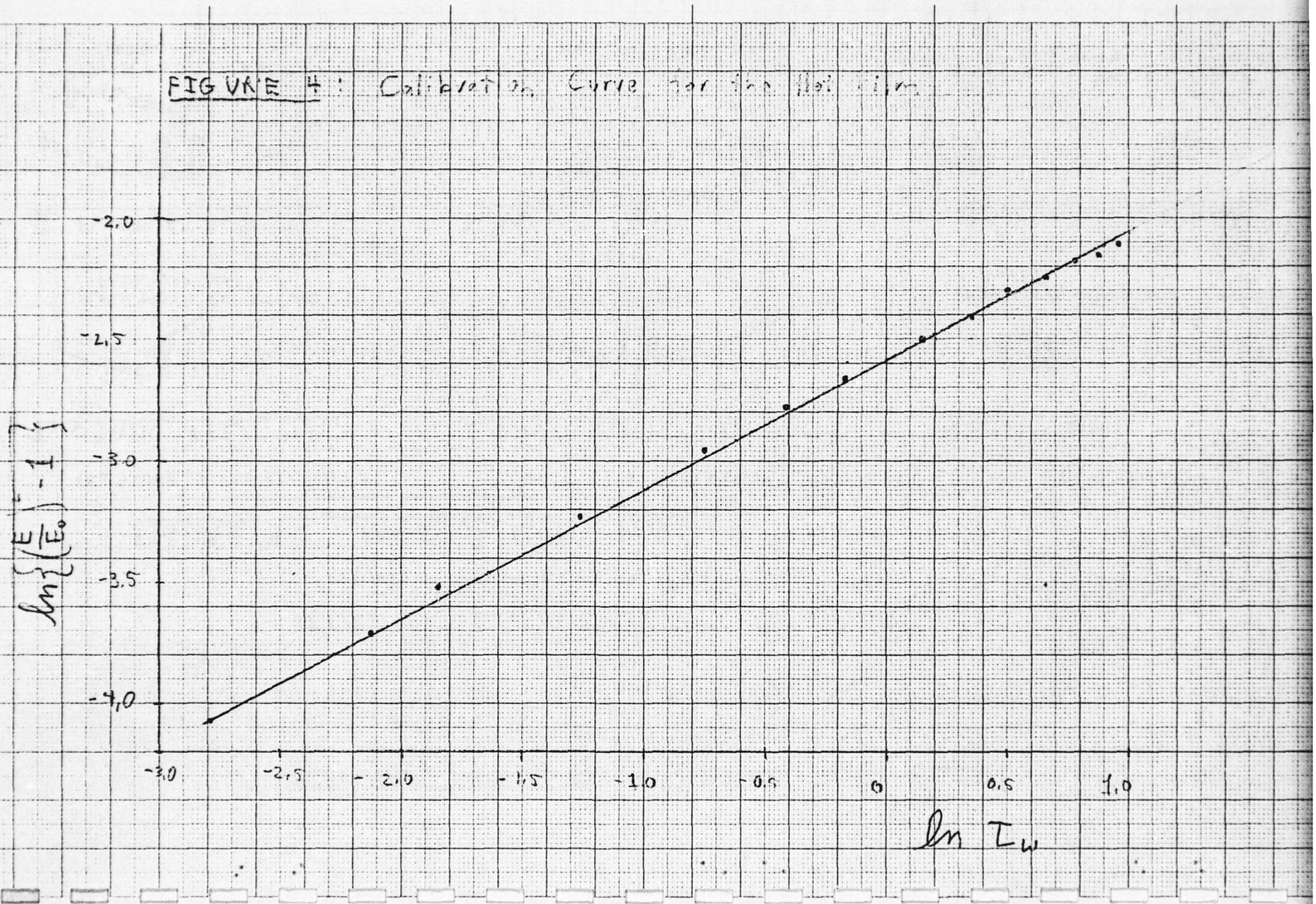

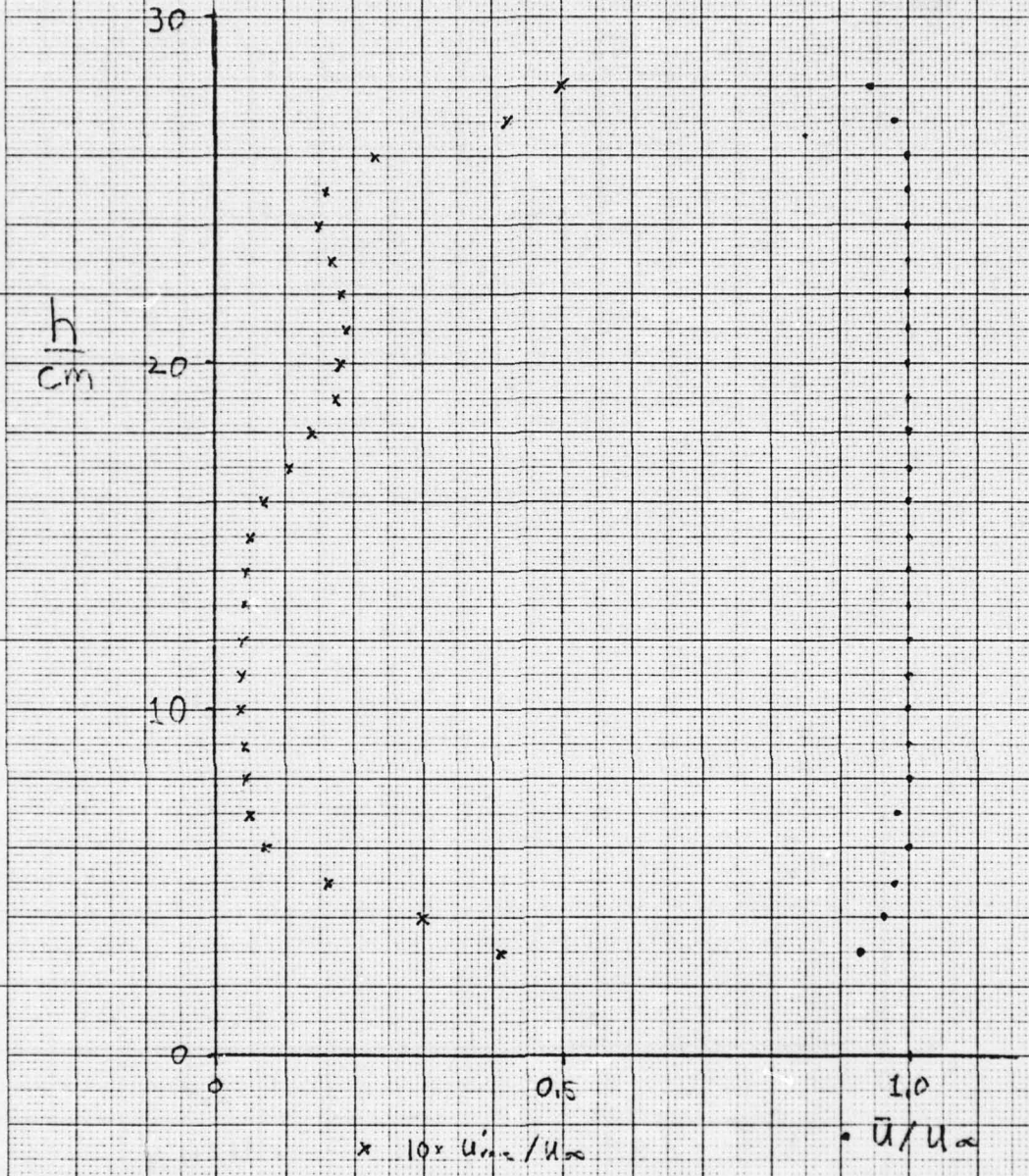


FIGURE 5 : Velocity Profile Across the Test Section for the Quiet Configuration

A4 210 x 297 mm
MADE IN GERMANY

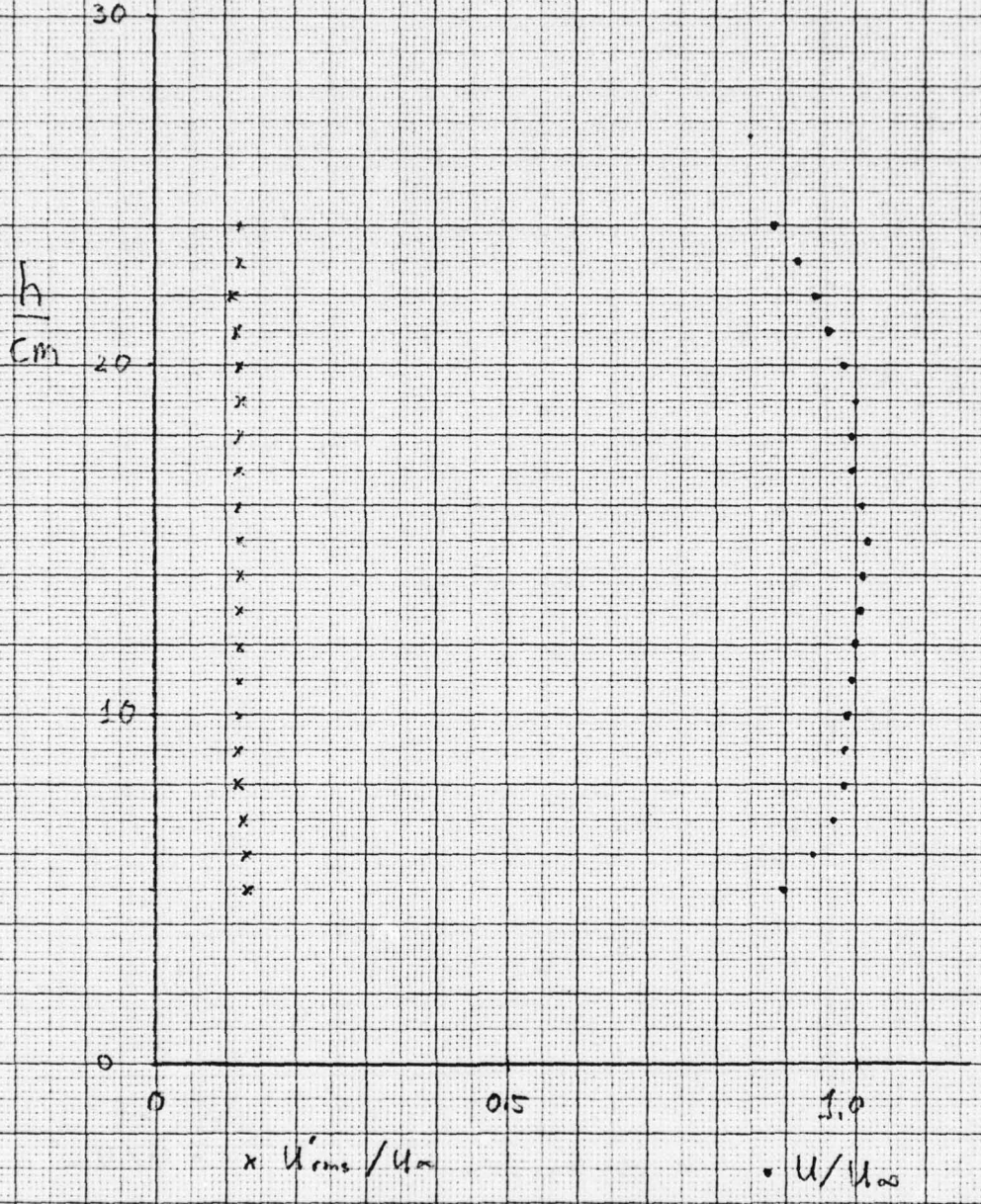


FIGURE 6: Velocity Profile Across the Test Section Behind the Turbulence Generating Grid

SELECTA A4 210 x 297 mm
MADE IN GERMANY

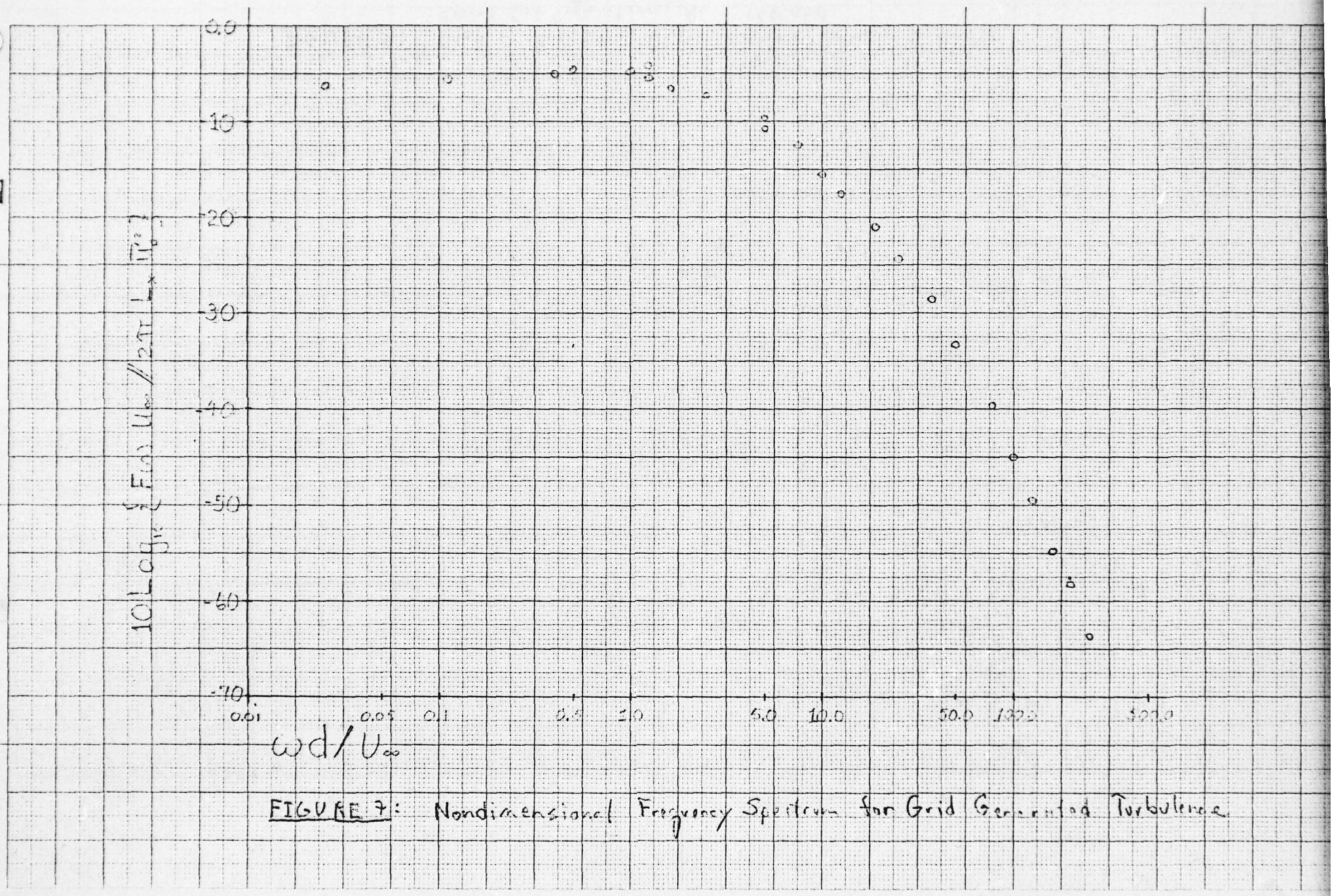


FIGURE 7: Nondimensional Frequency Spectrum for Grid Generated Turbulence

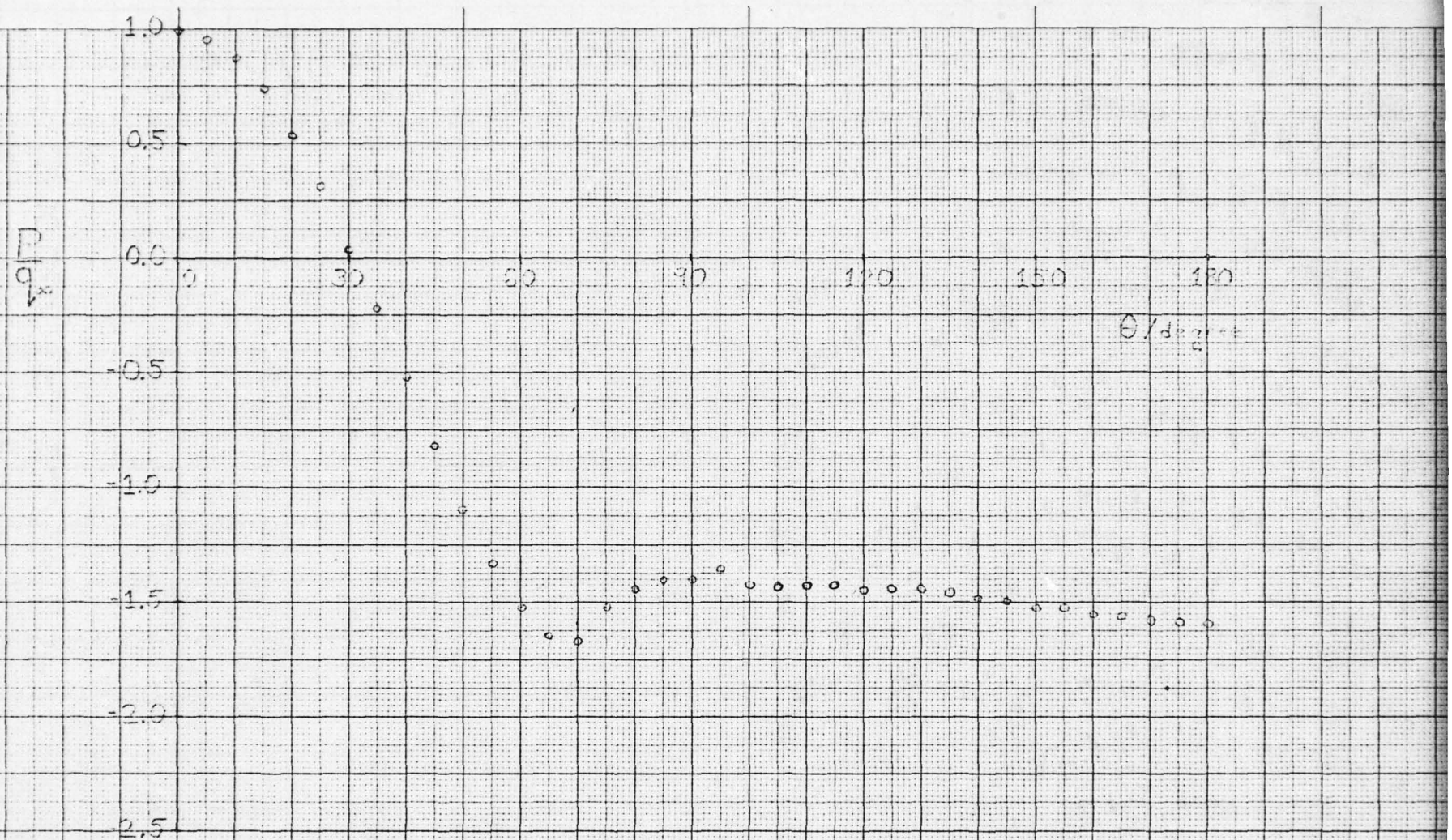


FIGURE 8: Static Pressure Distribution, Smooth Cylinder, Quiet Configuration, $Re = 106,000$

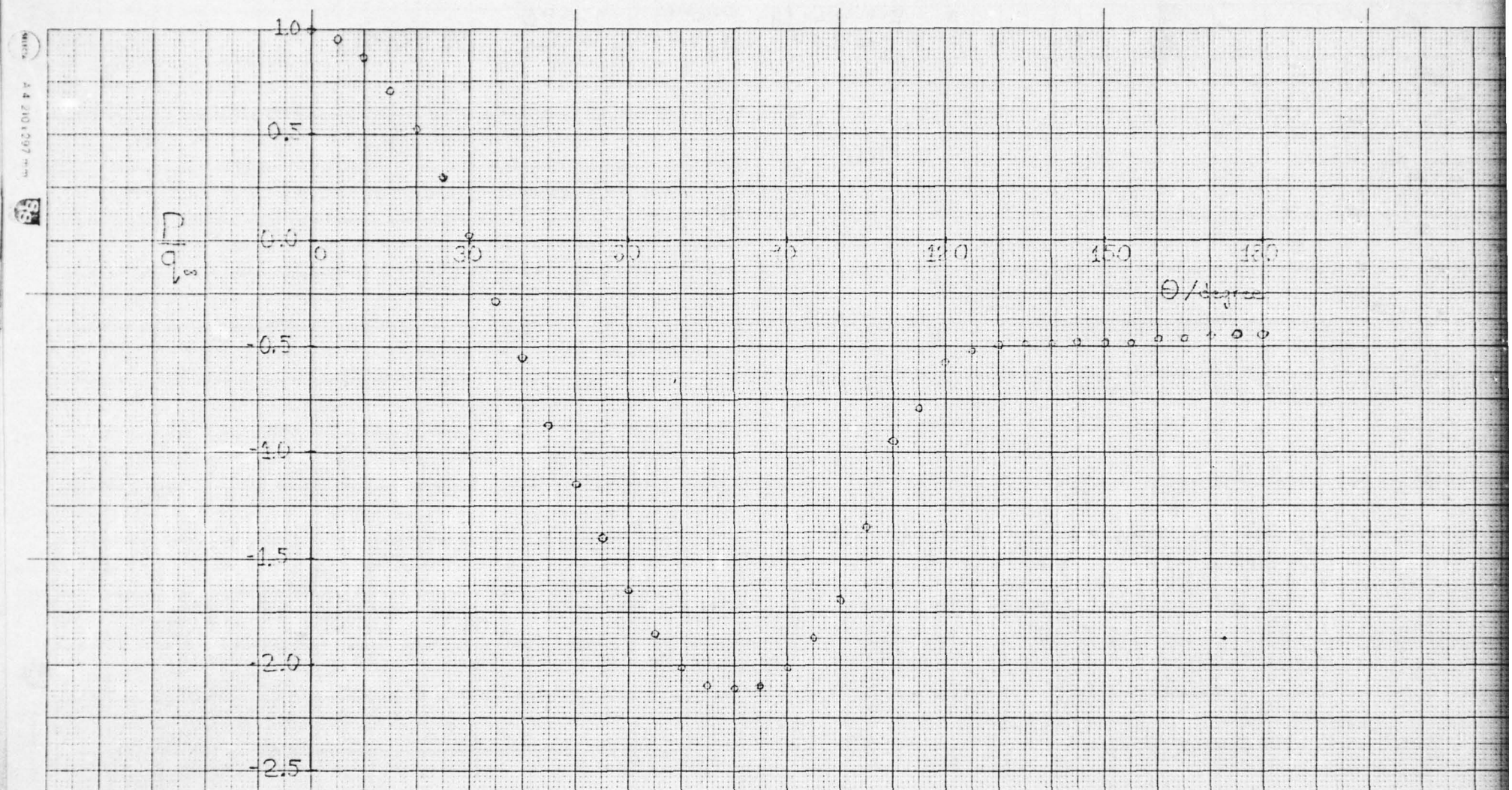


FIGURE 9: Static Pressure Distribution, Smooth Cylinder
Grid Generated Turbulence, $Re = 106,000$

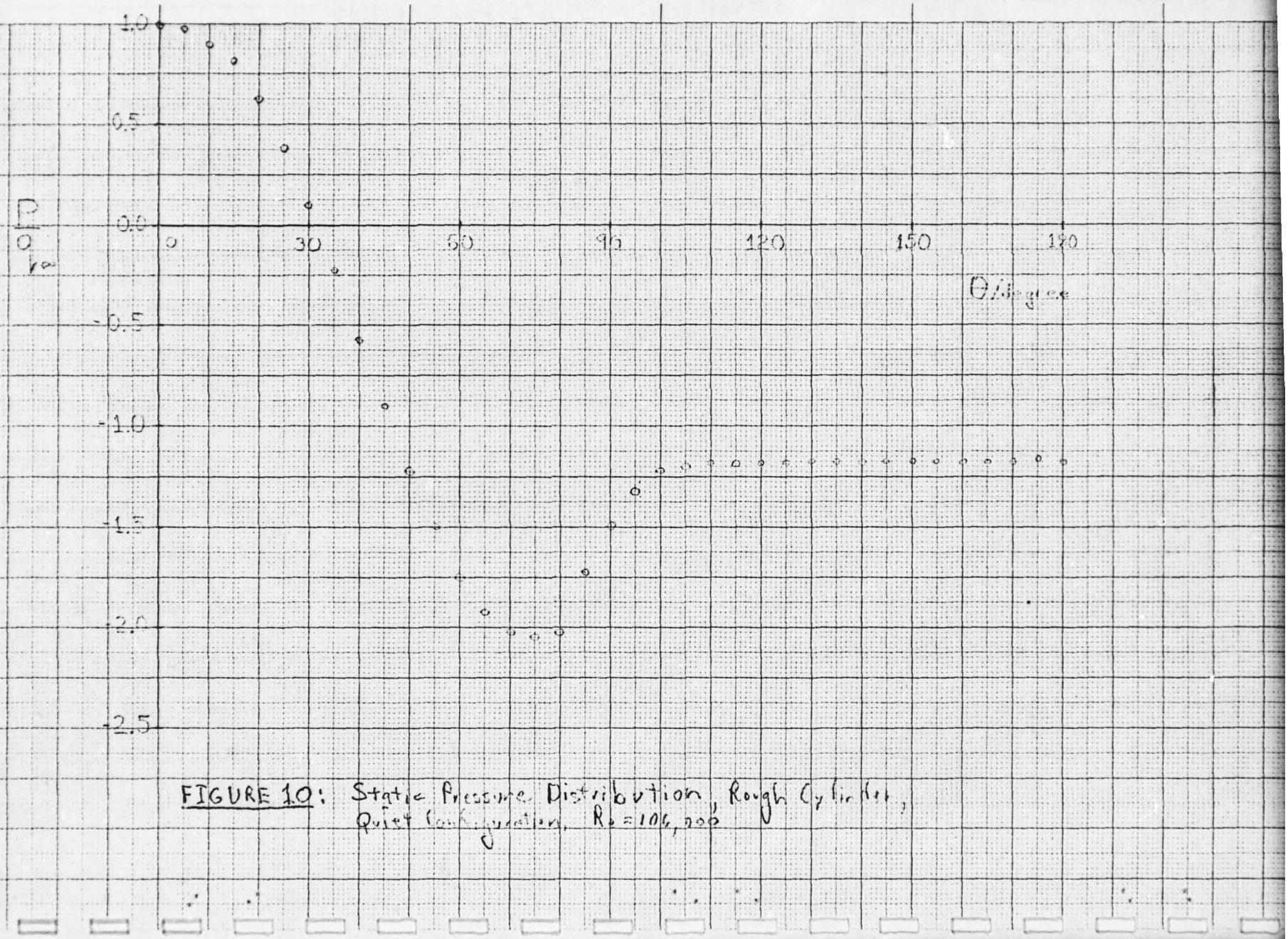


FIGURE 10: Static Pressure Distribution, Rough Cylinder, Quiet Tunnel Data, $R_d = 104,000$

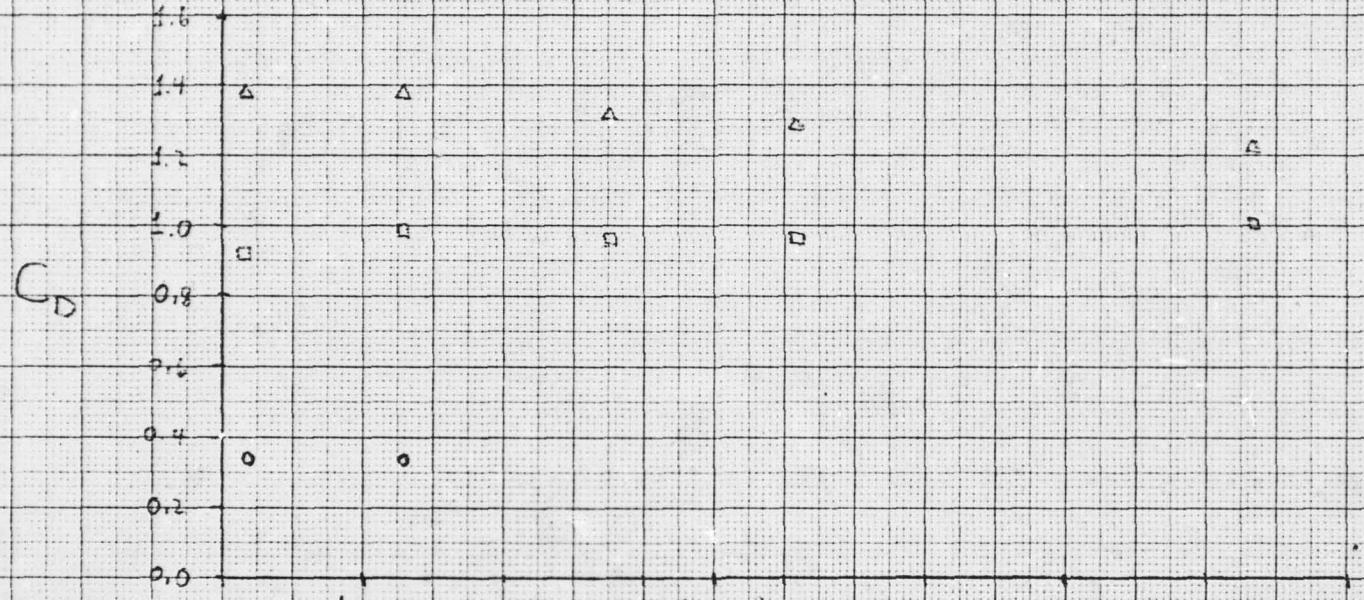


FIGURE 11 : Measured Values of Drag Coefficient

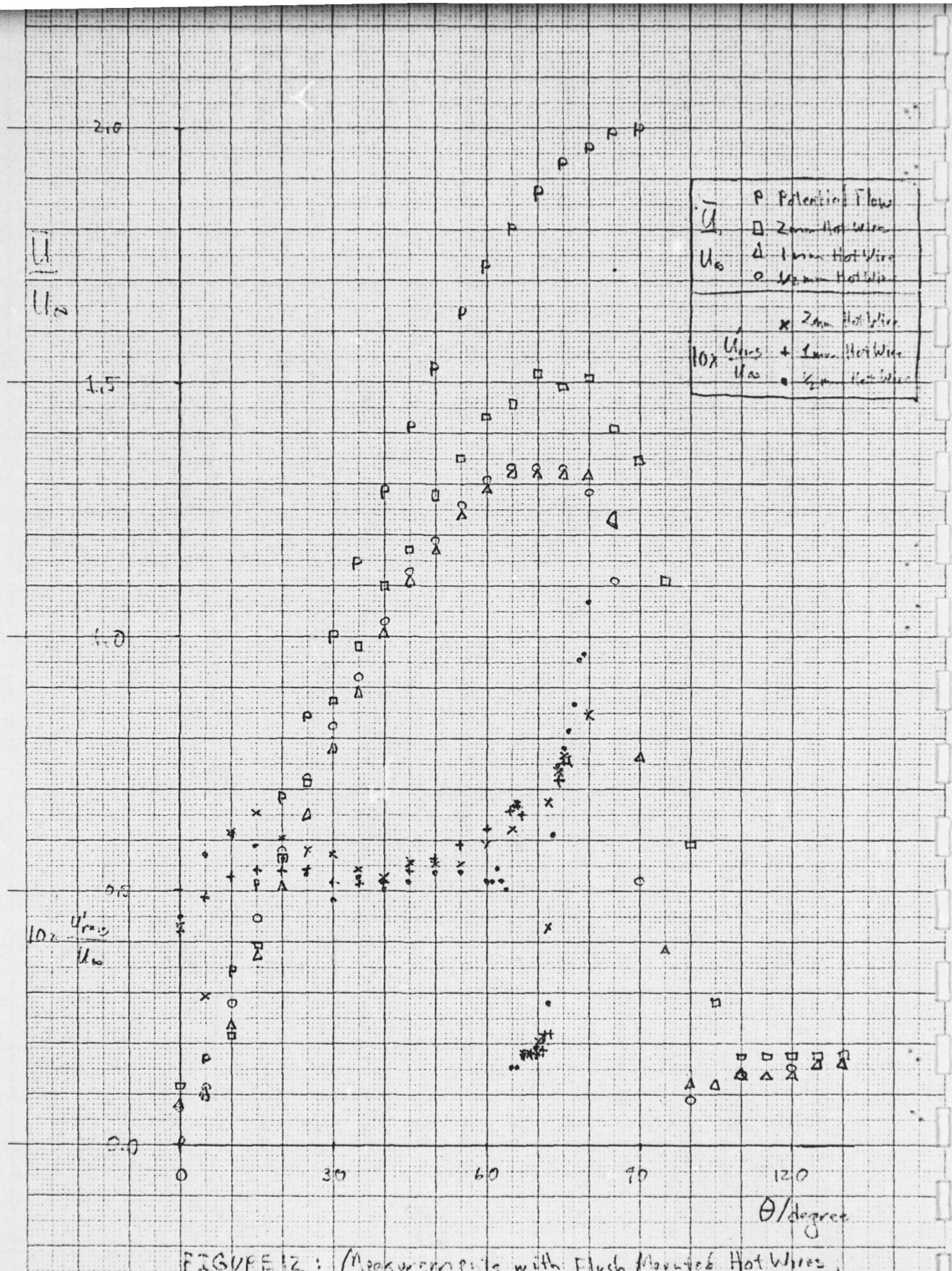


FIGURE 12 : Measurements with Flush Mounted Hot Wires, Smooth Cylinder, Quiet Tunnel.
$Re = 104,000$

A4 210x297 mm
MADE IN GERMANY

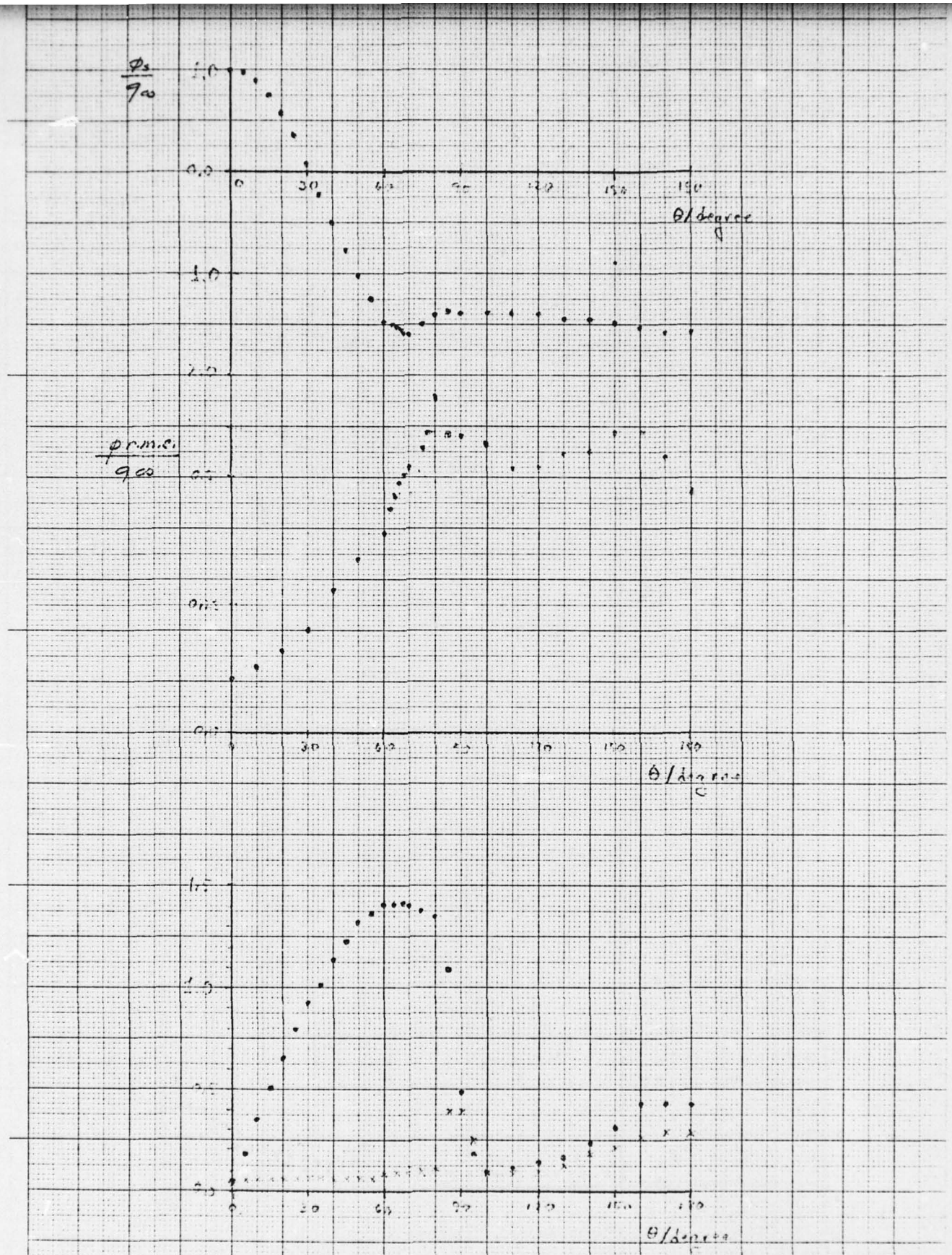


FIGURE 13 : Flow Measurements, Smooth Cylinder, Quiet Configuration, $Re = 93,000$

SELECTA A4 210 x 297 mm MADE IN GERMANY

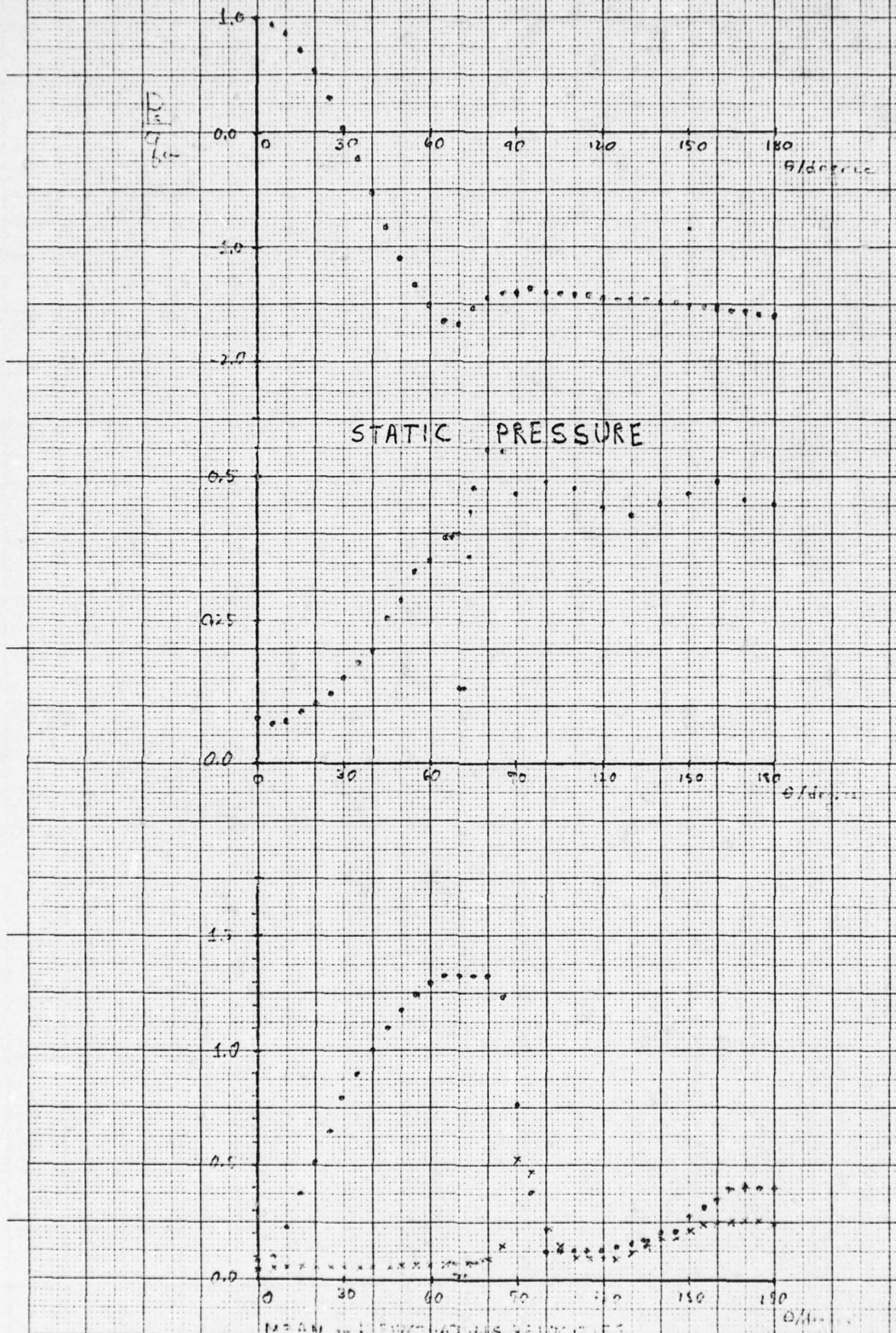


FIGURE 14: Flow Measurements Smooth Cylinder, Quiet Configuration, $R_d = 104,000$

A4 210 x 297 mm
MADE IN GERMANY

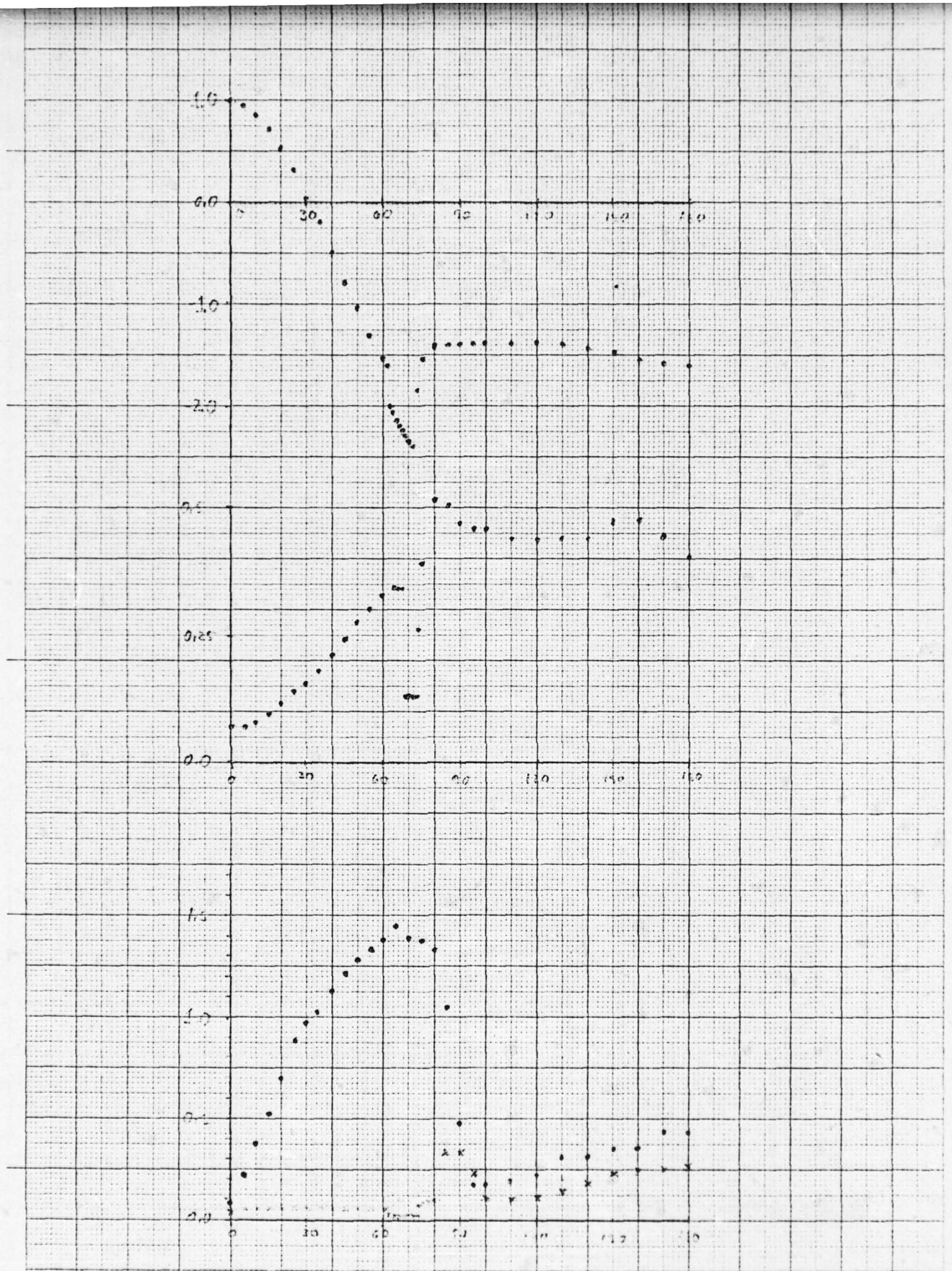

FIGURE 15: Flow Measurements, Smooth Cylinder, Quiet Conditions, $R_D = 117,000$

A4 210x297 mm

MADE IN GERMANY

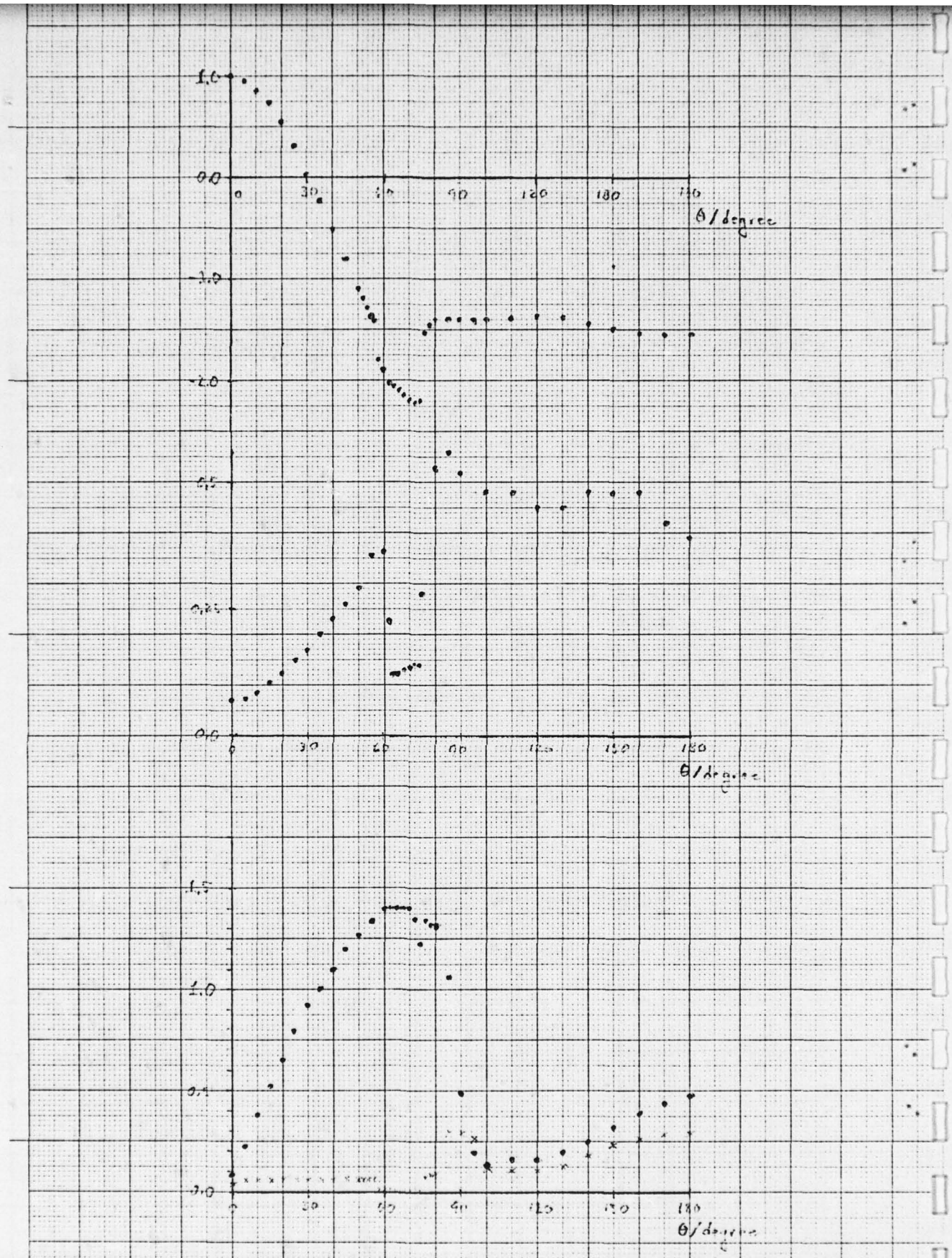


FIGURE 16: Flow Measurements, Smooth Cylinder, Quiet Configuration, Re = 132,000

SELECTA A 4 210 x 297 mm MADE IN GERMANY

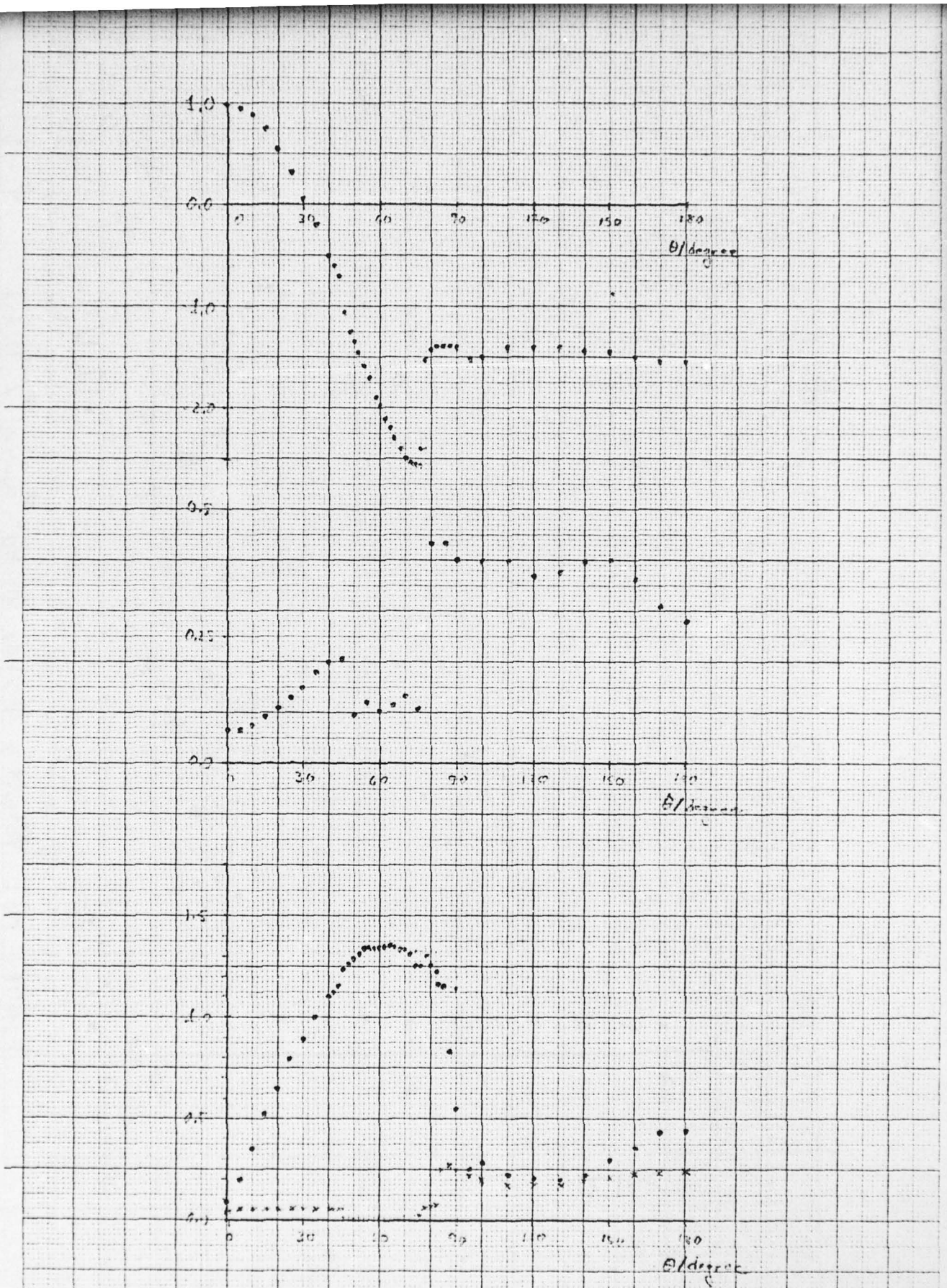


FIGURE 17: Flow Measurements, Smooth Cylinder, Quiet Conditions, $R_e = 167,000$

A 4 210 x 297 mm
MADE IN GERMANY

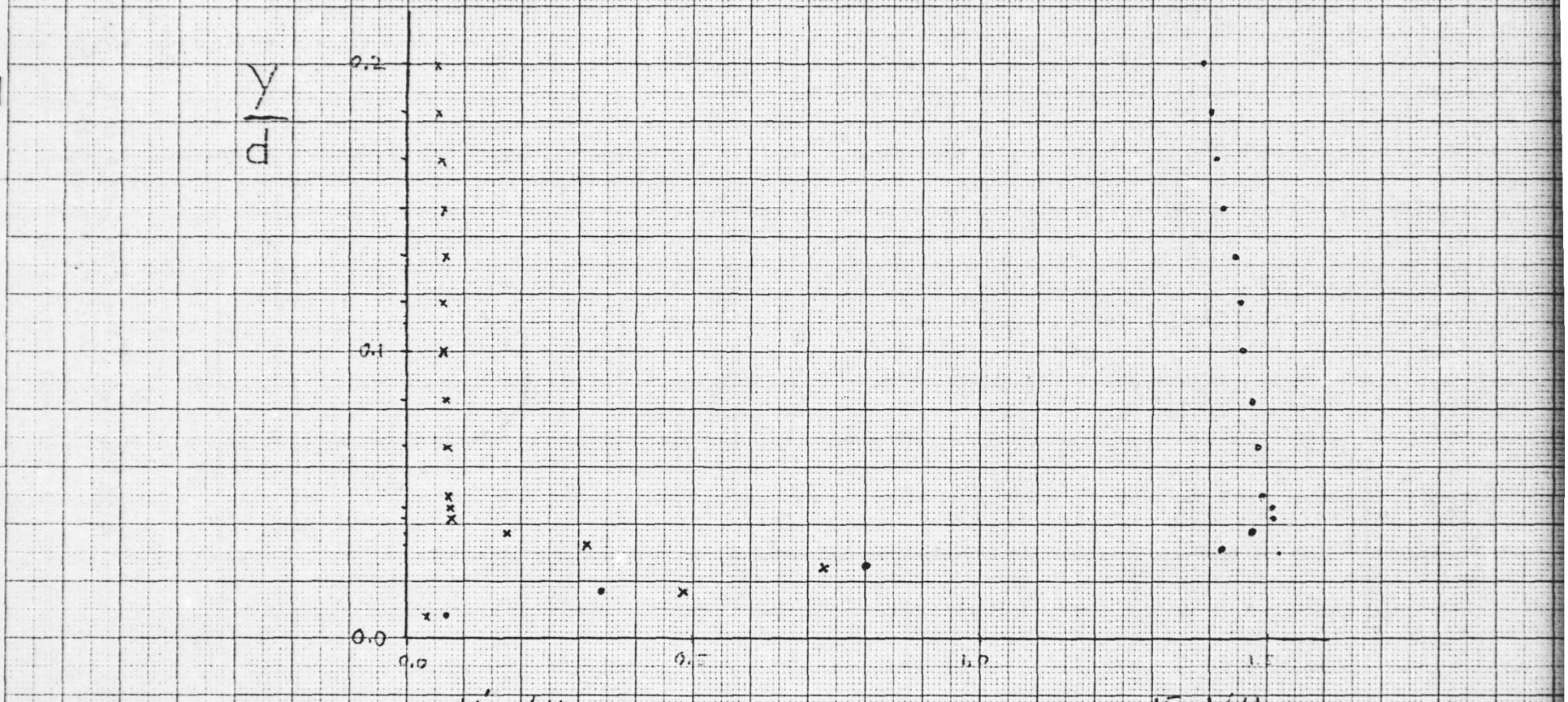


FIGURE 18: Velocity Profile at 90° Smooth Cylinder, Quiet Configuration, Re = 192,000

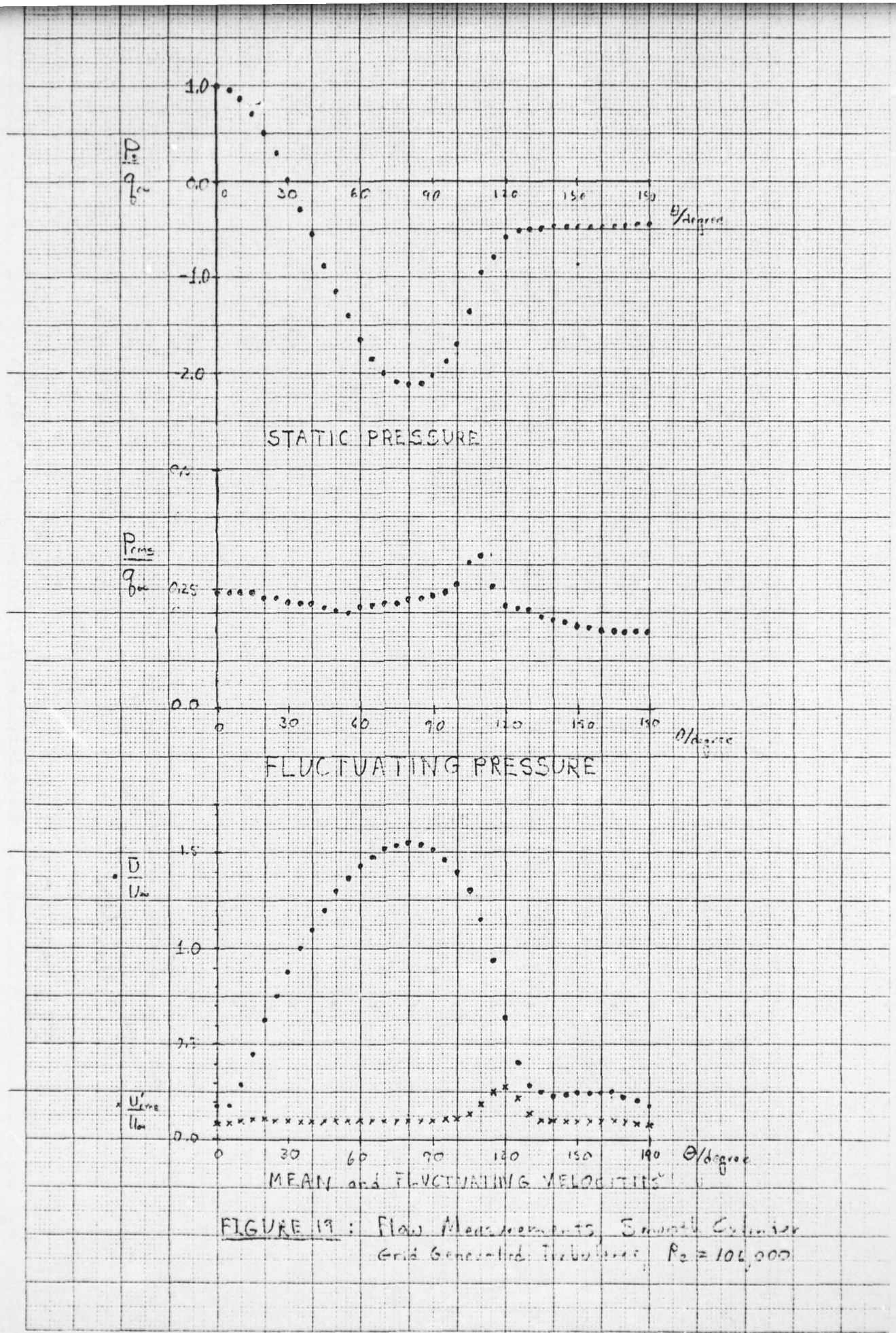


FIGURE 19 : Flow Measurements, Smooth Cylinder
Grid Generated Turbulence, $R_e = 104,000$

A 4 210 x 297 mm
MADE IN GERMANY

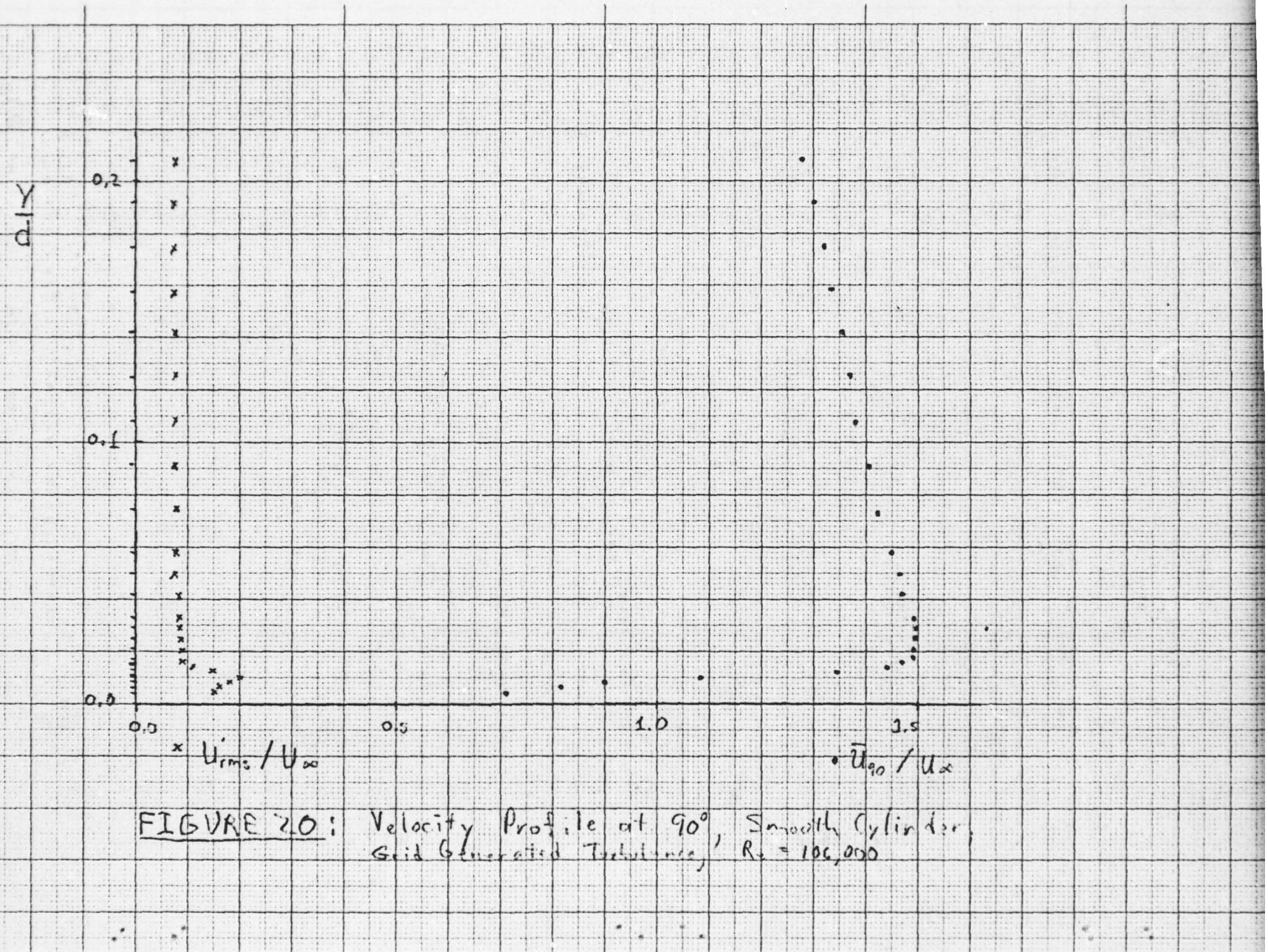


FIGURE 20: Velocity Profile at 90°, Smooth Cylinder, Grid Generated Turbulence, $R_e$ = 106,000

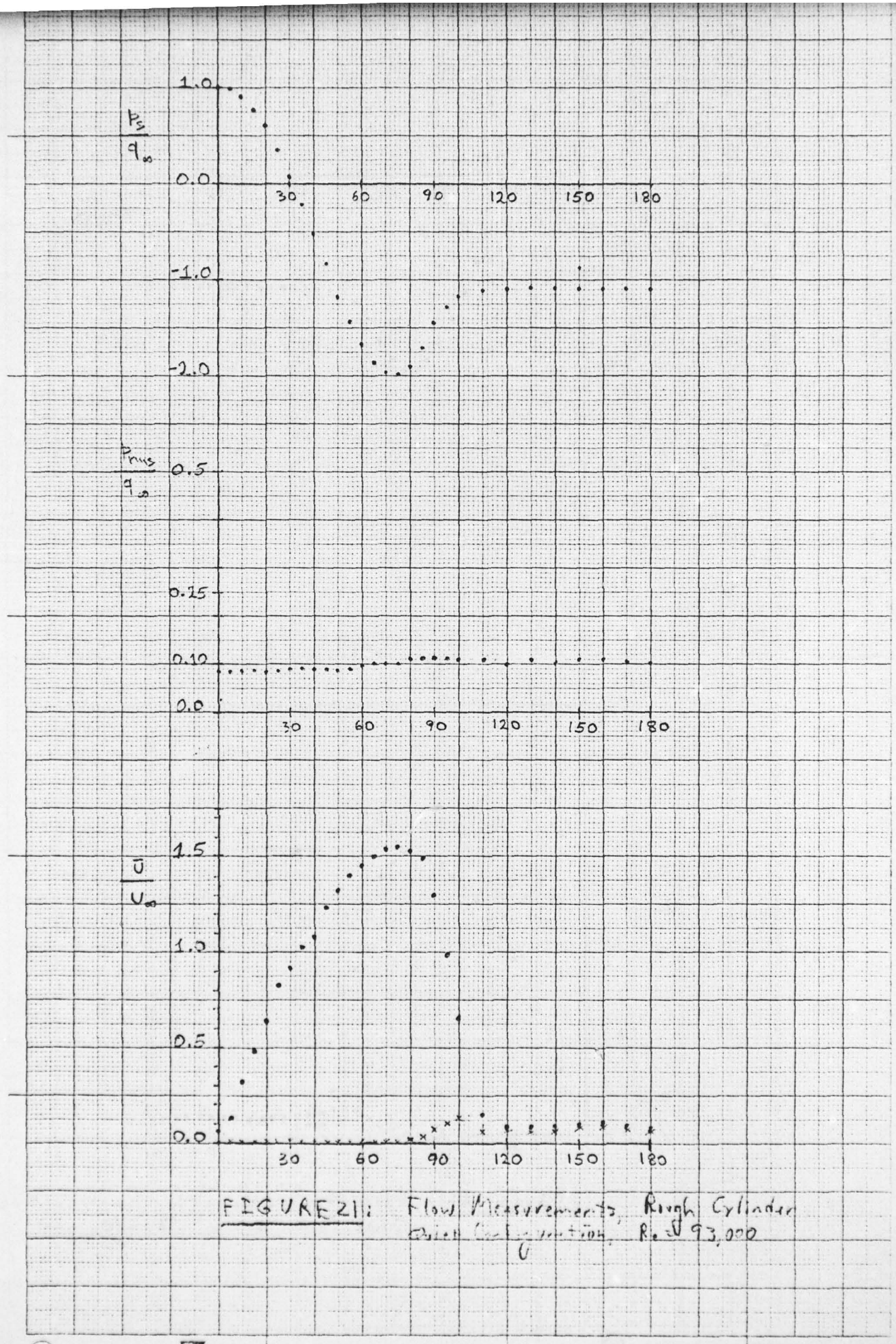


FIGURE 21: Flow Measurements, Rough Cylinder
Orientation, $R_e = 93,000$

SELECTA A4 210 x 297 mm
MADE IN GERMANY

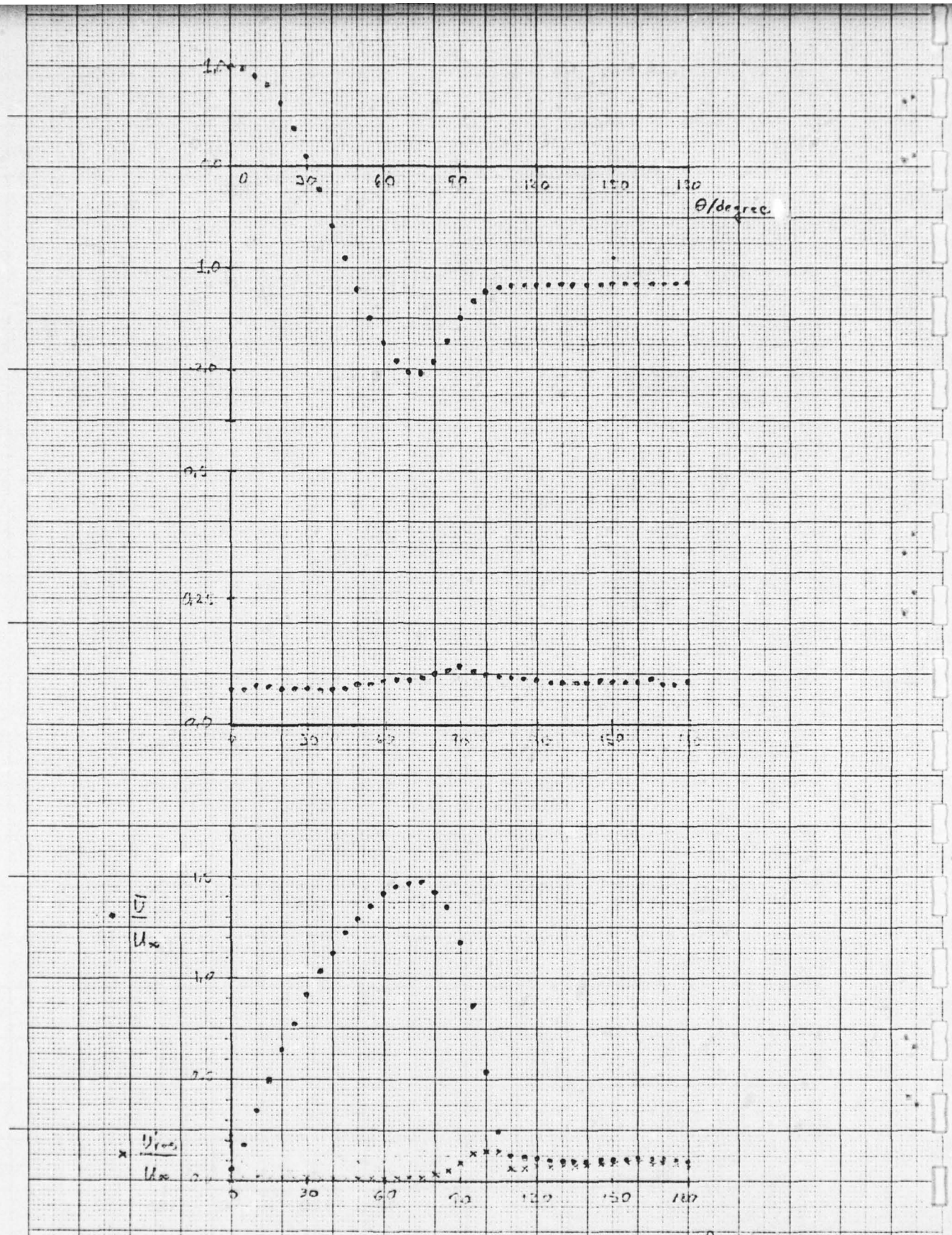


FIGURE 22: Flow Measurements; Rough Cylinder, Quiet Configuration, $R_D = 184,000$

A4 210 x 297 mm
MADE IN GERMANY

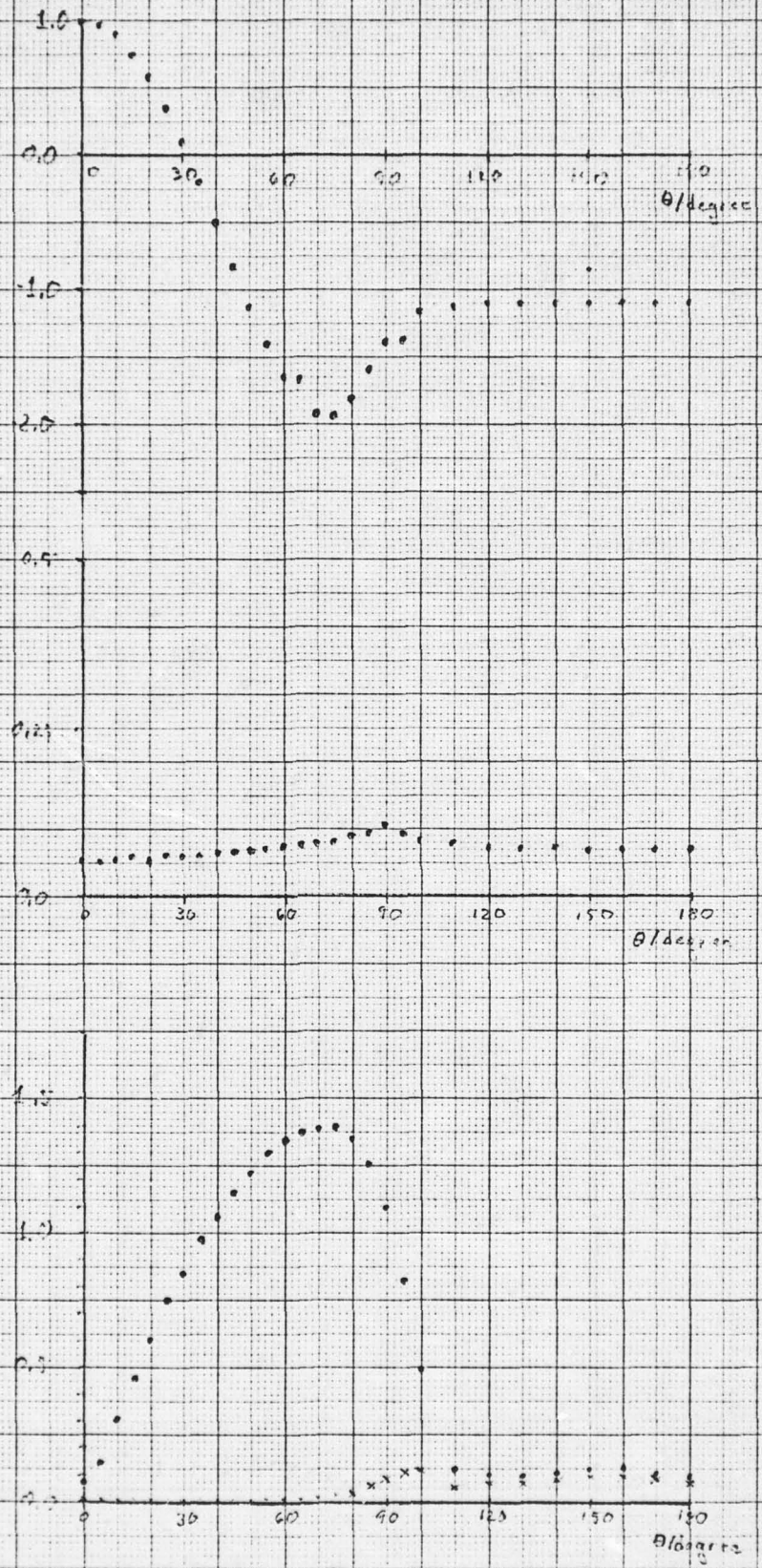


FIGURE 2.3 : Flow Measurements, Rough Cylinder Point Configurations, $R_e = 117,000$



A4 210 x 297 mm
MADE IN GERMANY

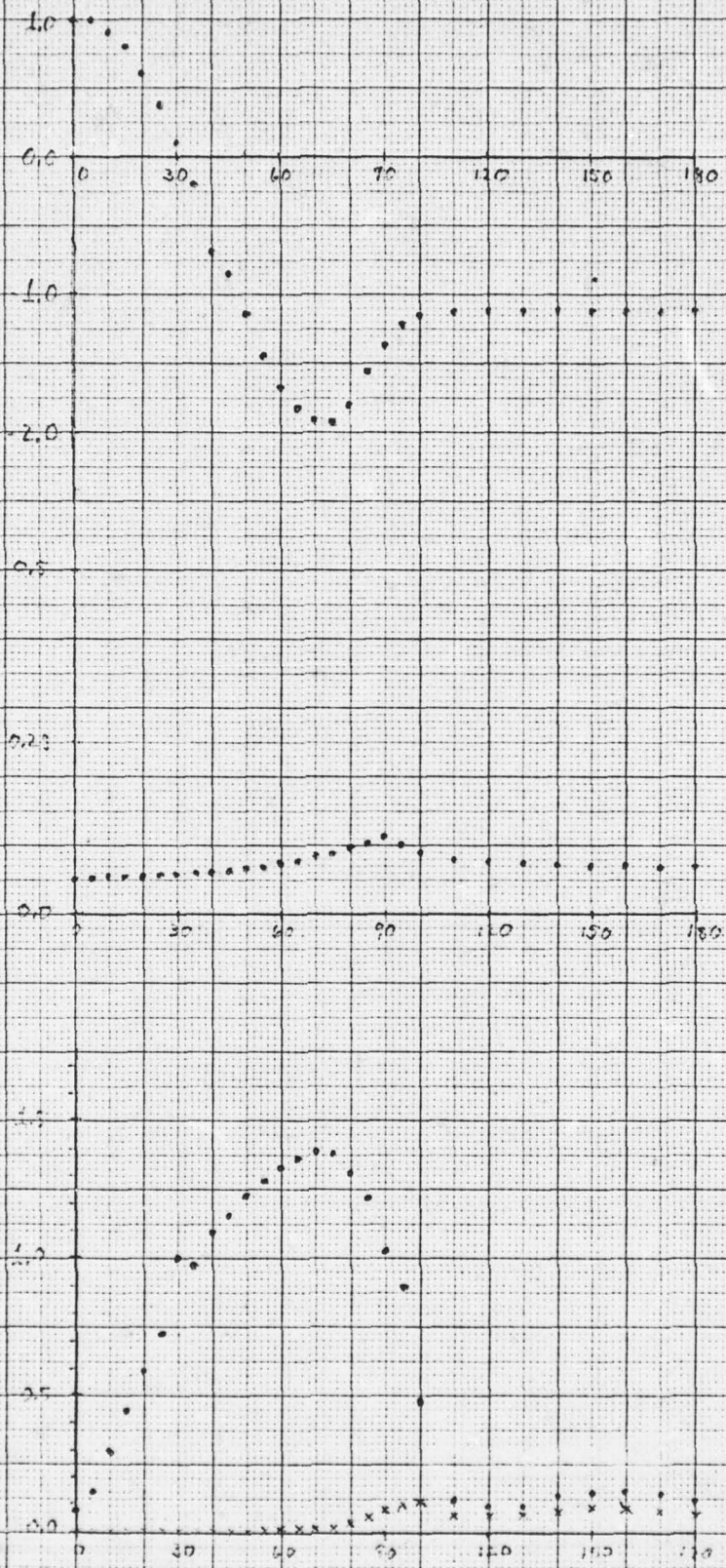


FIGURE 24: Flow Measurements, Rough Cylinder, Quiet Configuration, $Re_d$ 132,000

SELECTA A4 210x297 mm
MADE IN GERMANY

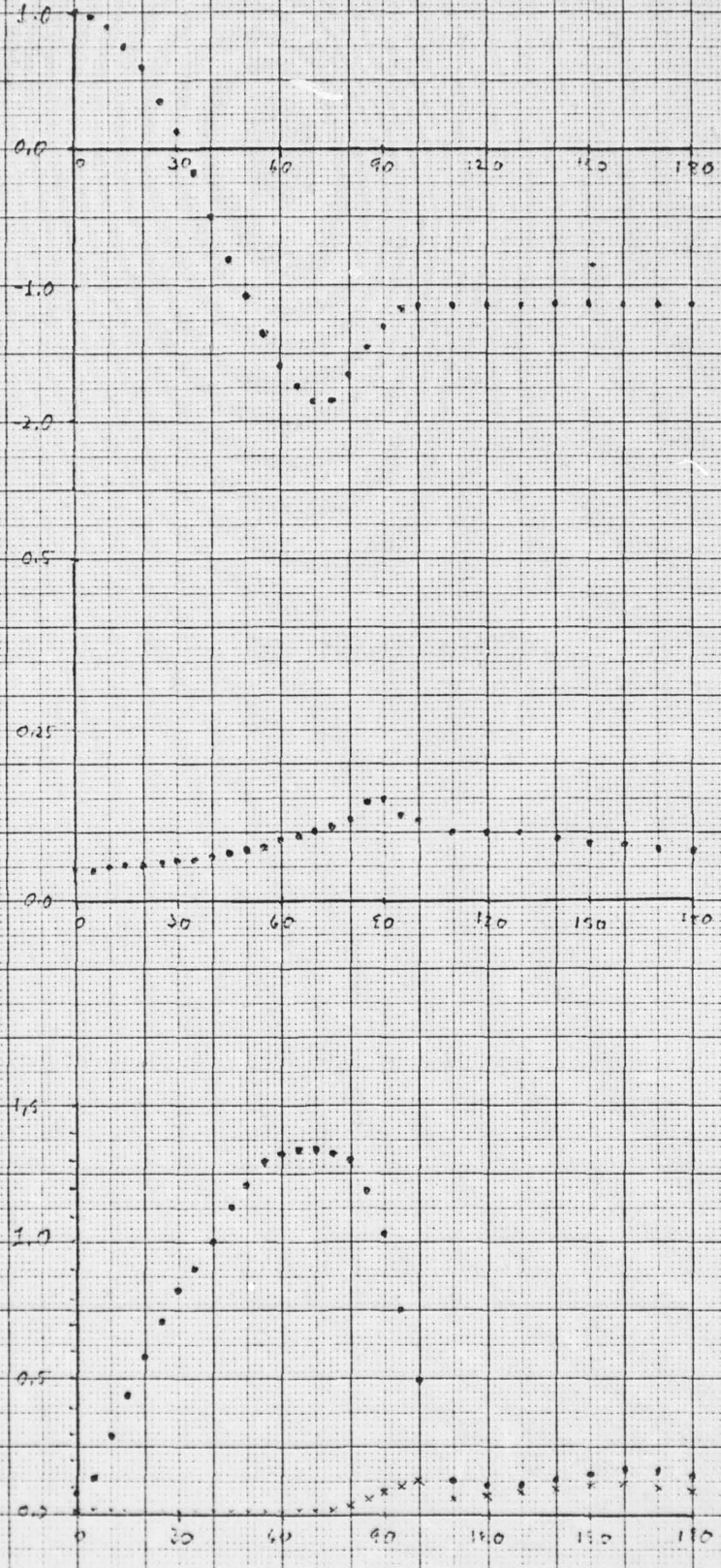


FIGURE 25: Flow Measurements, Rough Cylinder, Drier Configuration, $R_D = 17,000$

SELECTA A4 210 x 297 mm
MADE IN GERMANY

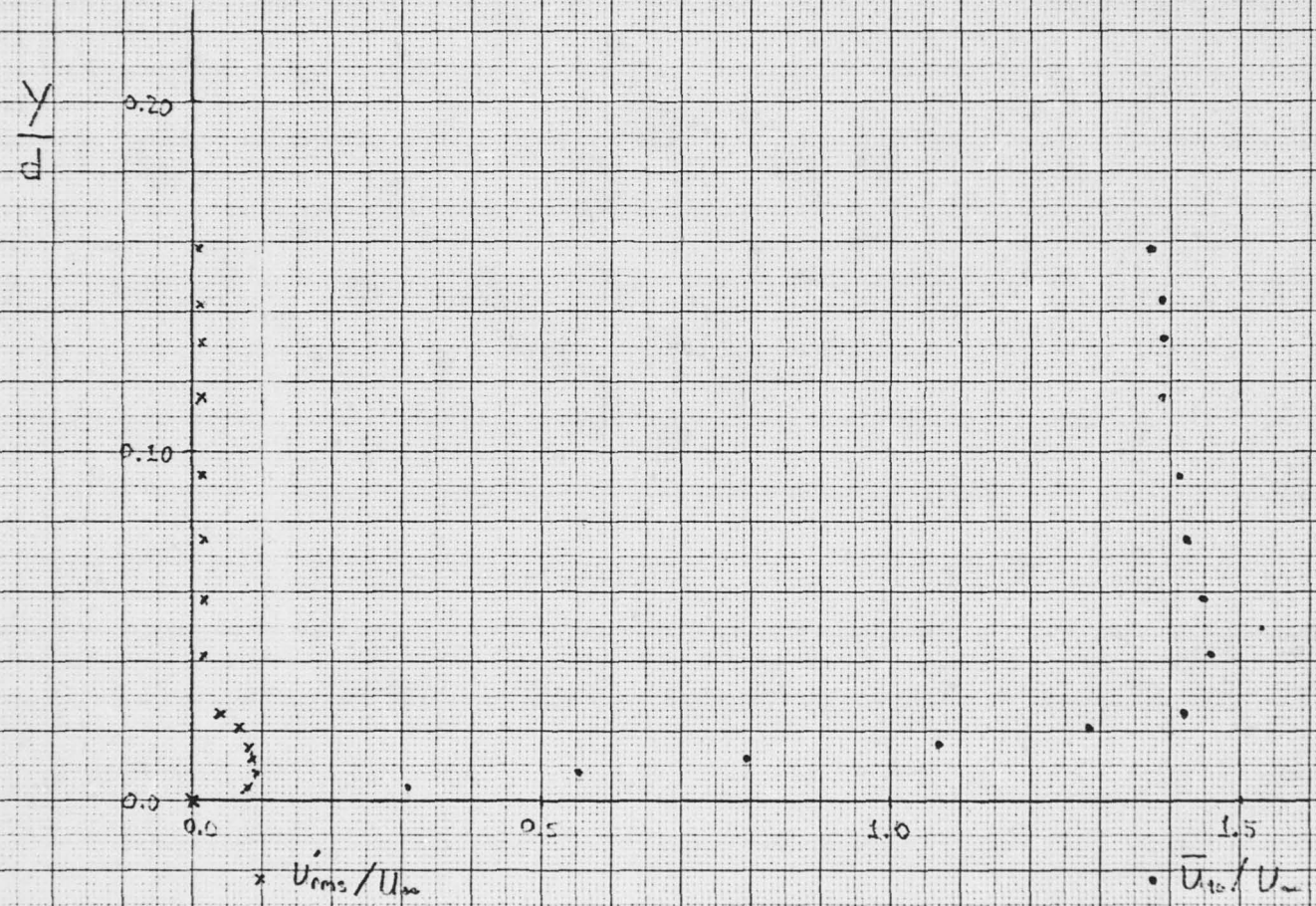


FIGURE 26 : Velocity Profile at 90°, Rough Cylinder, Quiet Configuration, Re = 104,000

FIGURE 27 Wall Shear Stress Measurements

$R_d$ = 73,000

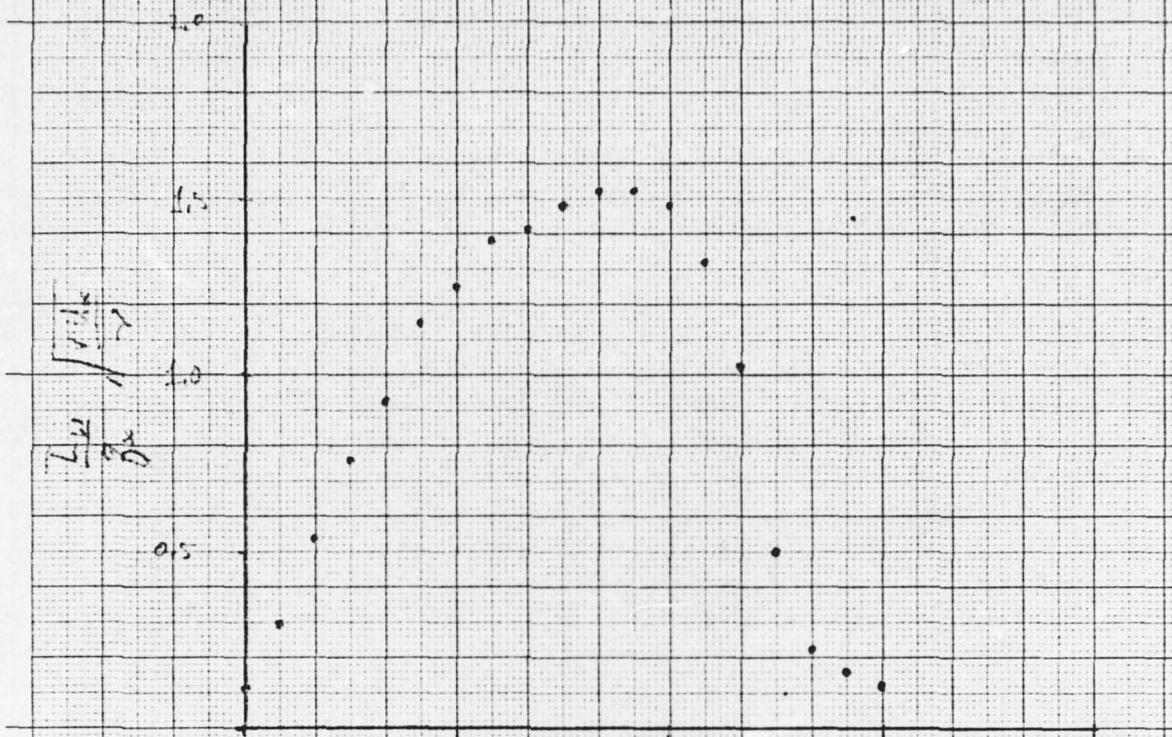


Smooth Cylinder

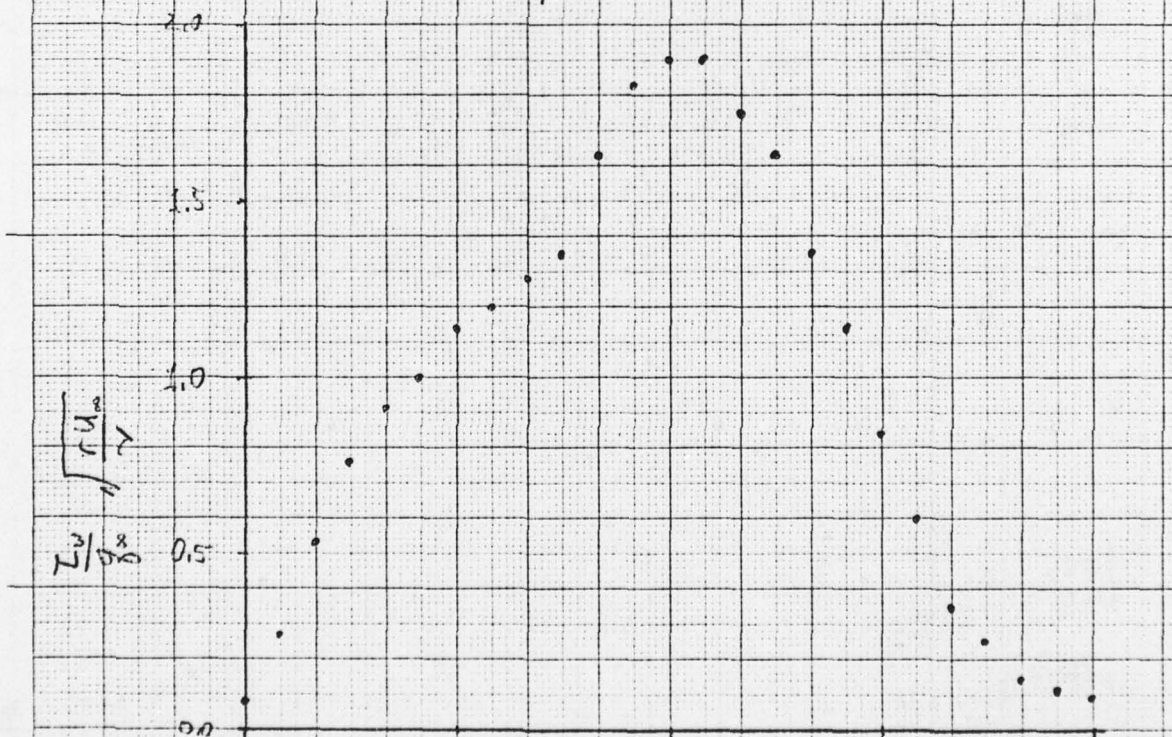


Rough Cylinder

SELECTA A 4 210 x 297 mm MADE IN GERMANY

FIGURE 28 : Wall Shear Stress Measurements,
$R_e = 106,000$

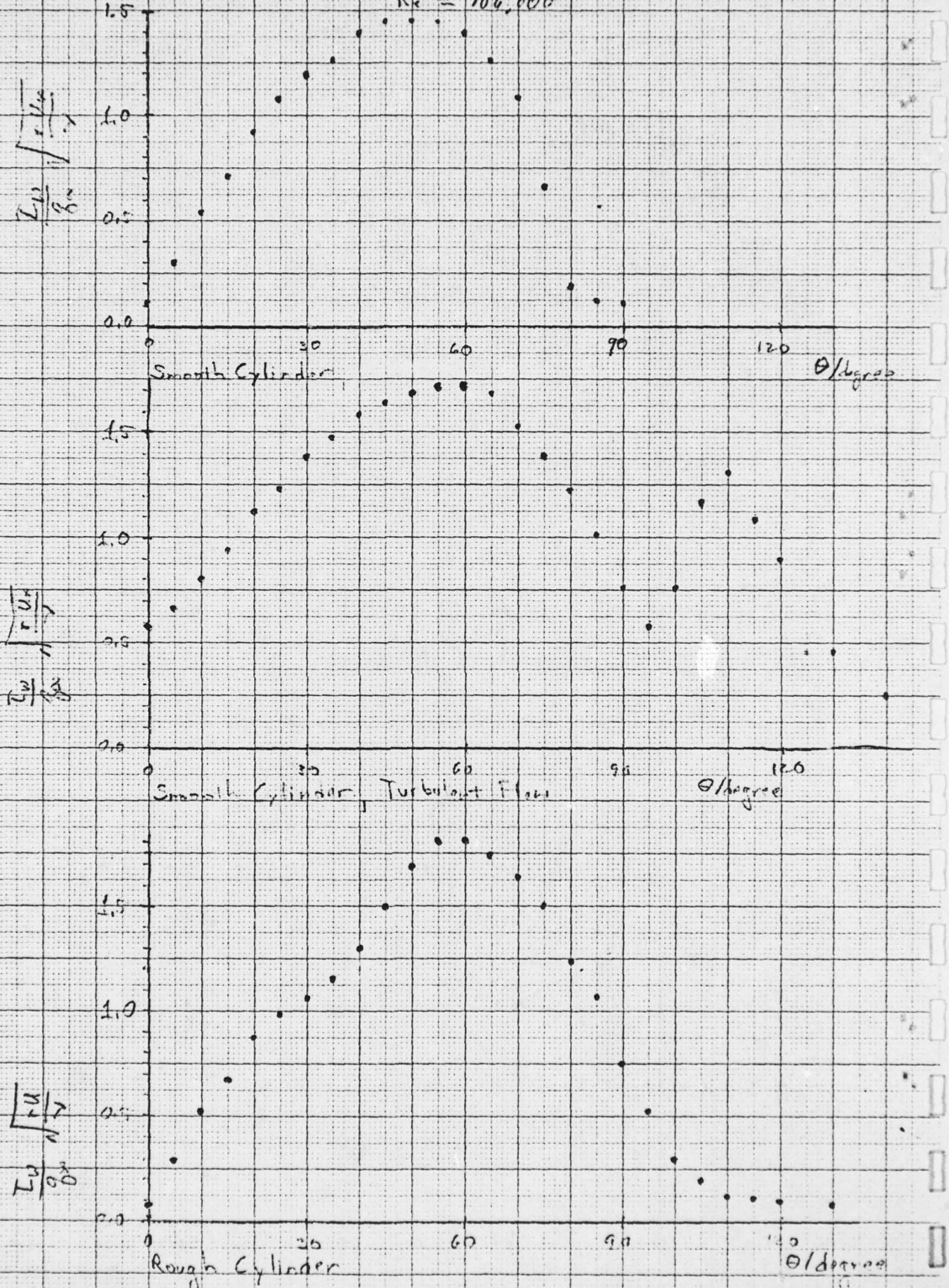


A 4 210 x 297 mm
MADE IN GERMANY

FIGURE 29 : Wall Shear Stress Measurements, $R_\ell = 117,000$

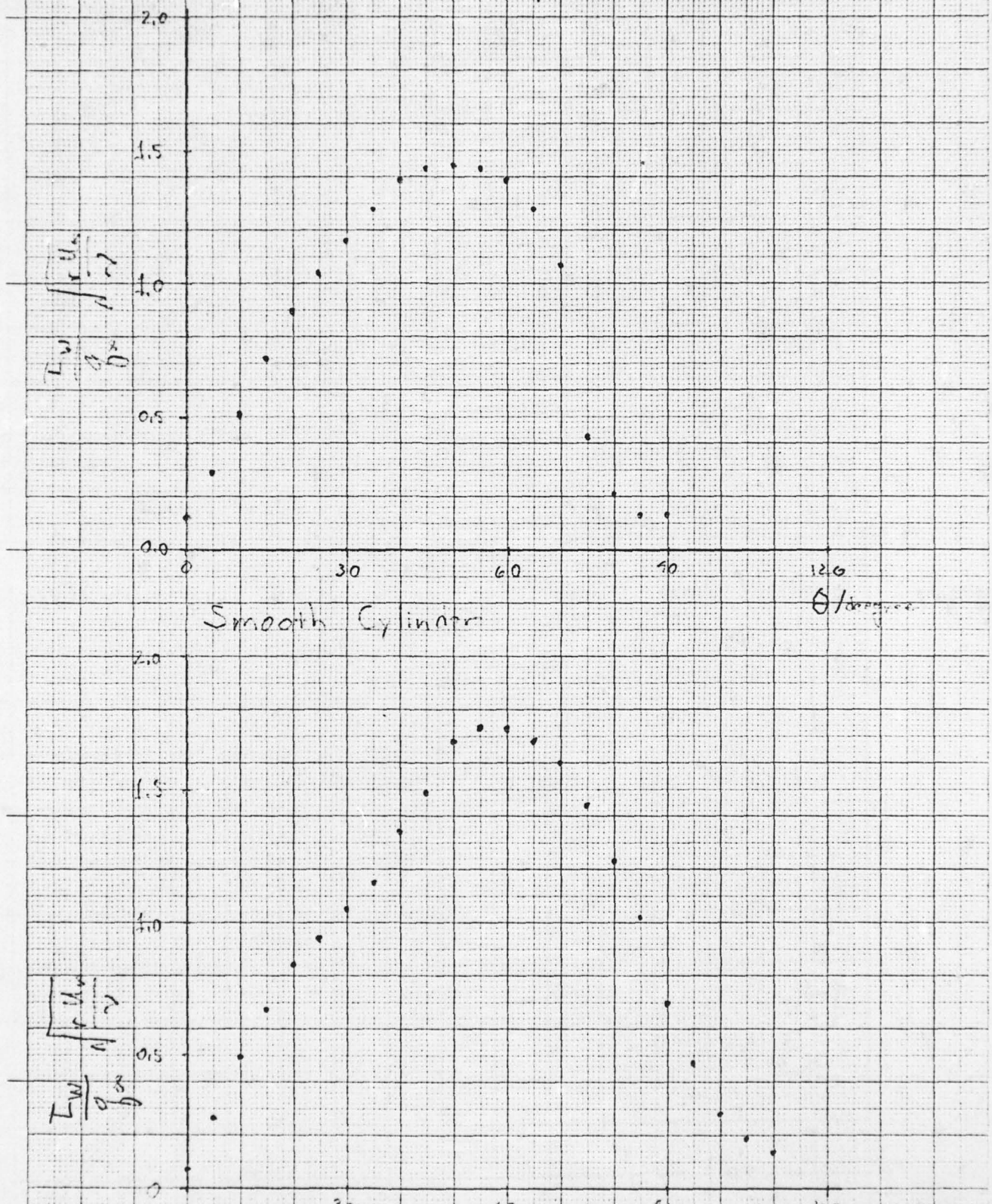


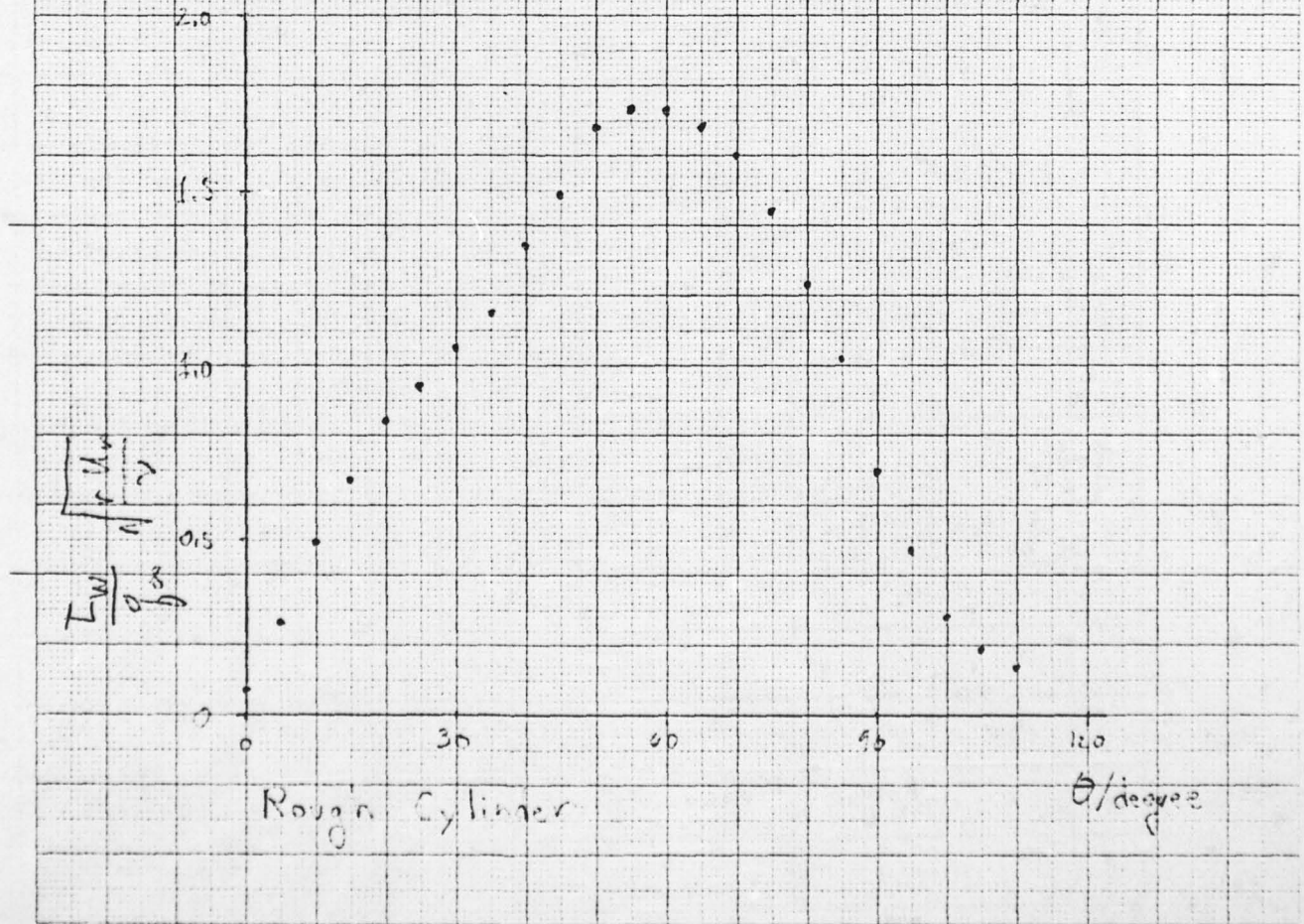


A4 210 x 297 mm
MADE IN GERMANY

FIGURE 20: Wall Shear Stress Measurements, $R_e$ = 132,000

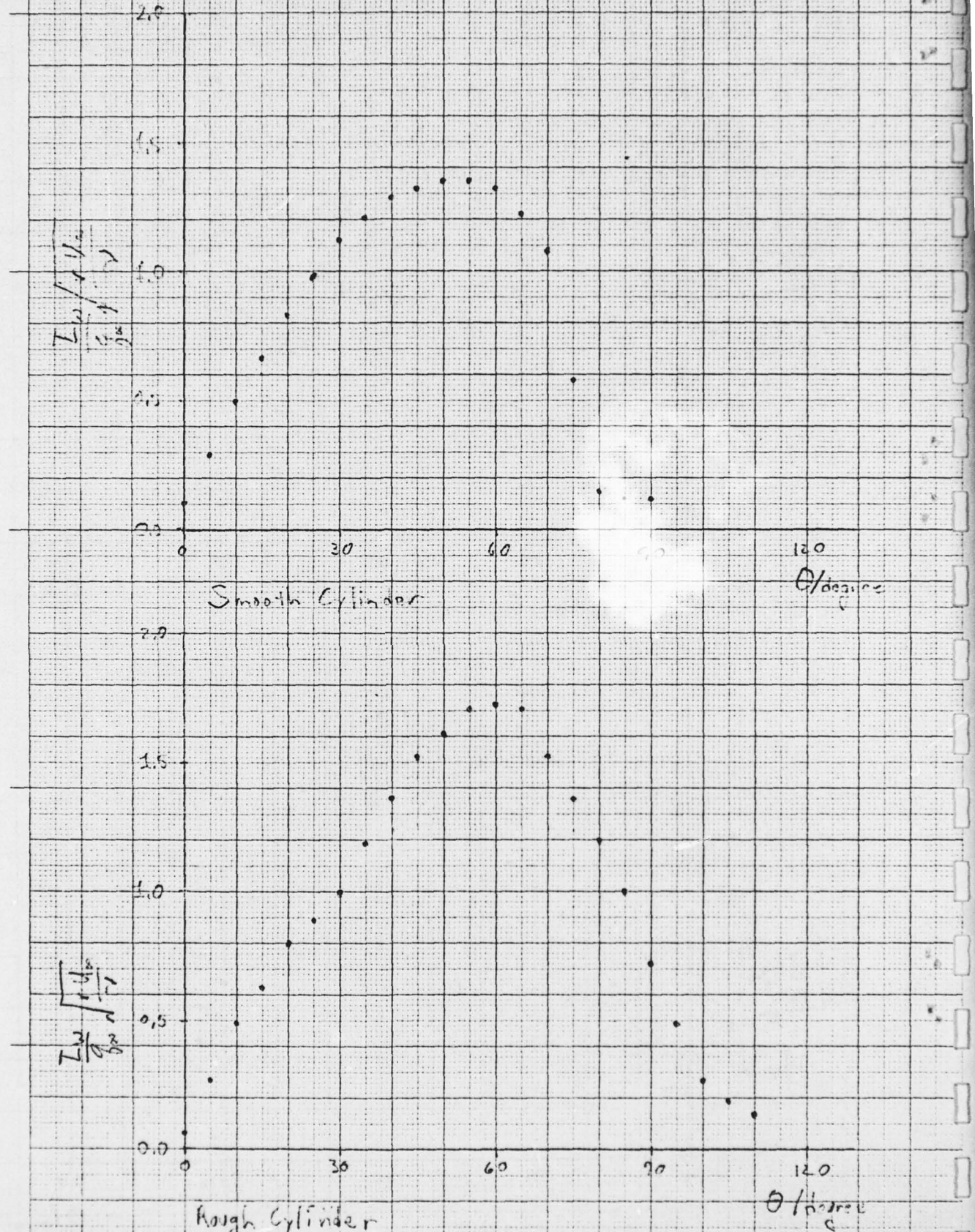


A 4 210 x 297 mm
MADE IN GERMANY

FIGURE 31: Wall Shear Stress Measurements, Re = 167,000

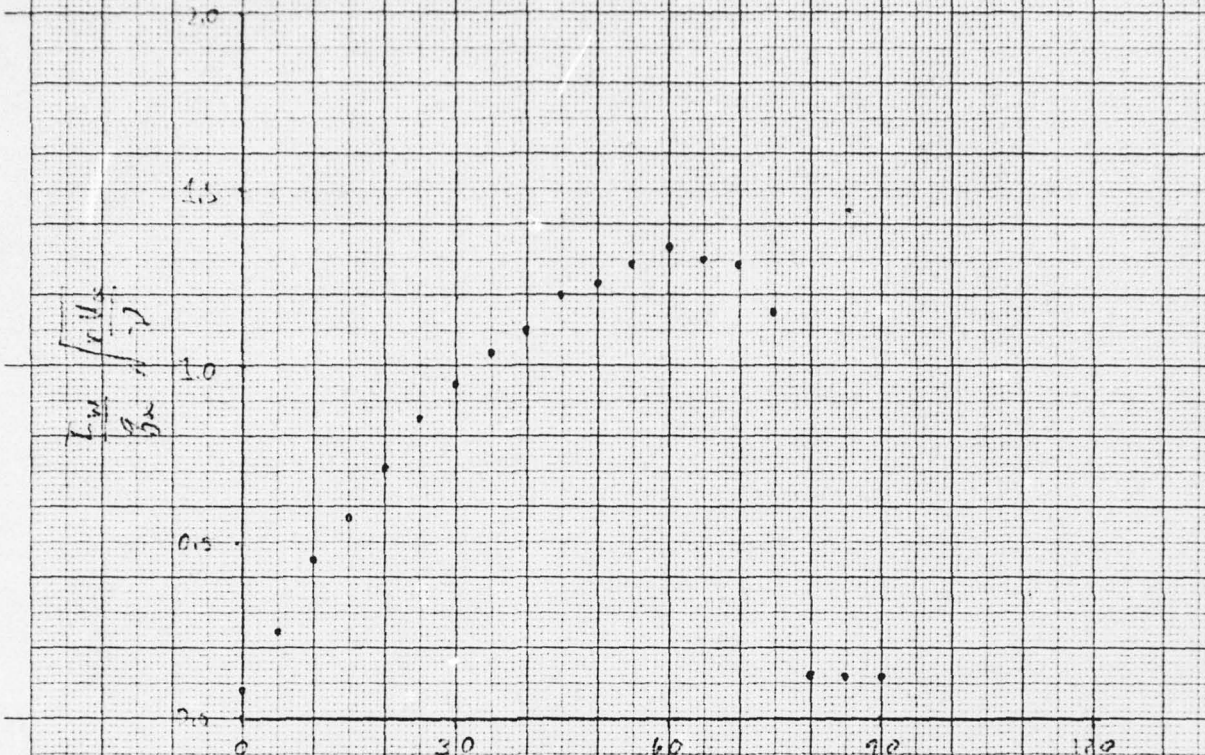


Smooth Cylinder

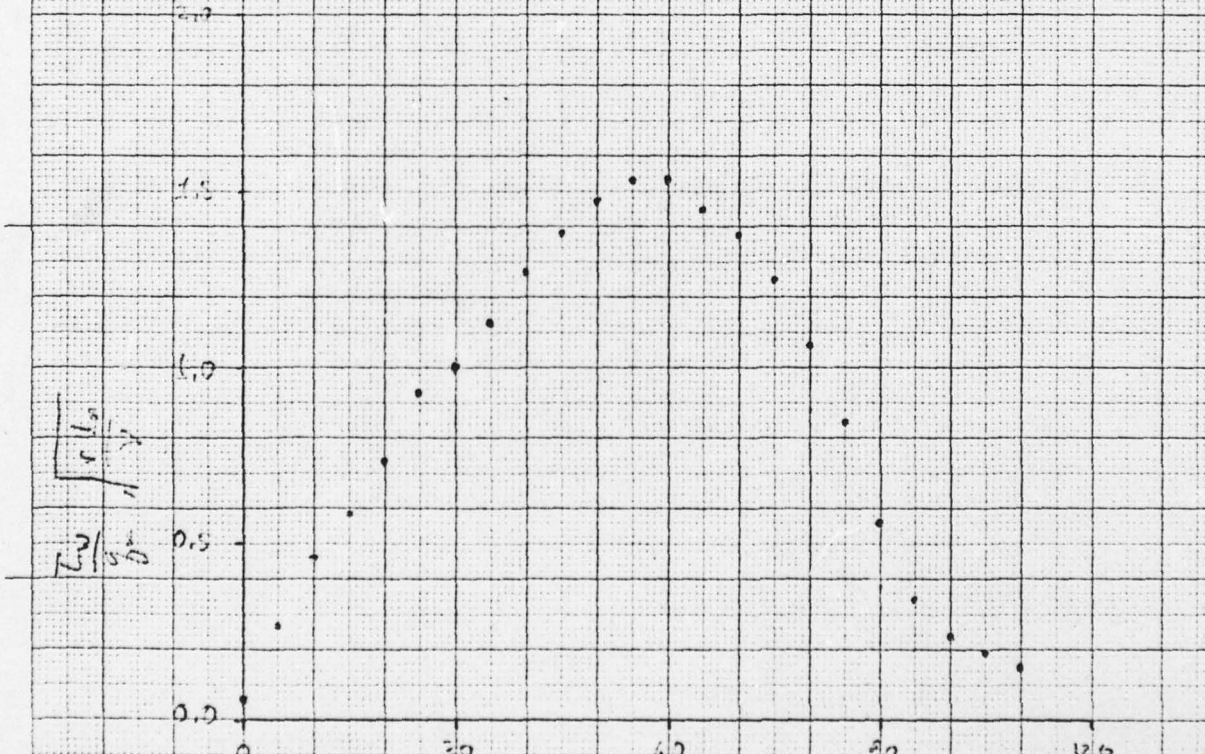


Rough Cylinder

A4 210 x 297 mm
MADE IN GERMANY